

GEORGIA DOT RESEARCH PROJECT 23-16

Final Report

**ADVANCED 5.9GHZ INTERFERENCE
RESILIENCY FOR CONNECTED VEHICLE
EQUIPMENT**



Office of Performance-based Management and Research
600 West Peachtree Street NW | Atlanta, GA 30308

March 2025

TECHNICAL REPORT DOCUMENTATION PAGE

1. Report No.: FHWA-GA-25-2316		2. Government Accession No.: N/A		3. Recipient's Catalog No.: N/A	
4. Title and Subtitle: Advanced 5.9GHz Interference Resiliency for Connected Vehicle Equipment			5. Report Date: March 2025		
			6. Performing Organization Code: N/A		
7. Author(s): Billy Kihei (PI), Ph.D. (https://orcid.org/0000-0002-0426-3145) Graduate Researcher; James Grow Undergraduate Research Assistants; Nakira Oglesby, Mackenzie Prescott, Grayson Hatcher, Marco Tello, Sam Amoah, Khason Murphy, William Walker, Anthony Iwejuo			8. Performing Organization Report No.: 23-16		
9. Performing Organization Name and Address: Kennesaw State University 840 Polytechnique Lane Marietta, GA 30060 Phone: (470) 578-6657 Email: bkihei@kennesaw.edu			10. Work Unit No.: N/A		
			11. Contract or Grant No.: PI#0019918		
12. Sponsoring Agency Name and Address: Georgia Department of Transportation (SPR) Office of Performance-based Management and Research 600 West Peachtree St. NW Atlanta, GA 30308			13. Type of Report and Period Covered: Final; (March 2024 – March 2025)		
			14. Sponsoring Agency Code: N/A		
15. Supplementary Notes: Prepared in cooperation with the U.S. Department of Transportation, Federal Highway Administration.					
16. Abstract: In this work the research team reports on the effectiveness of various techniques to mitigate Wi-Fi 5 interference on Vehicle-to-Everything communications and provide a means to reliably detect Wi-Fi 5 interference. Following previous work conducted in RP 22-18, the research team performed three research investigations in this new work. The first investigation discovered the minimum guard band size needed between aged low-cost real-world Wi-Fi 5 devices is 15MHz. This results in a recommendation to set policies for Wi-Fi 5 devices near connected vehicle roadside units. The second investigation discovered a passive in-line radio frequency hardware configuration to reduce the effect of Wi-Fi 5 interference, while not degrading the performance of Vehicle-to-Everything communications. The results provide a recommendation including a prototype in-line treatment that can work with the existing roadside unit configurations and the roadside unit stock 5.9GHz antennas. The third investigation discovered a method to utilize software defined radio technology to detect and measure the amount of Wi-Fi 5 interference near a roadside unit. This resulted in an interference detection kit that a technician or cognizant connected vehicle engineer can utilize to perform a war drive through roadside unit installation locations in order to detect and measure the amount of Wi-Fi 5 interference without hiring a third party.					
17. Keywords: Intelligent Transportation Systems, Connected Vehicle, Wireless, Communications, DSRC, IEEE 802.11p, U-NII-4, Wireless Interference			18. Distribution Statement: No Restriction		
19. Security Classification (of this report): Unclassified	20. Security Classification (of this page): Unclassified	21. No. of Pages: 60	22. Price: Free		

GDOT Research Project 23-16

Final Report

ADVANCED 5.9GHZ INTERFERENCE RESILIENCY FOR CONNECTED VEHICLE
EQUIPMENT

By

Billy Kihei, Ph.D.
Professor¹

James Grow
Graduate Researcher¹

Nakira Oglesby, Grayson Hatcher, Sam Amoah,
William Walker, Anthony Iwejuo, Marco Tello,
Mackenzie Prescott, Khason Murphy
Undergraduate Researcher¹

¹Kennesaw State University
Department of Electrical and Computer Engineering

Kennesaw State University Research and Service Foundation, Inc.

Contract with
Georgia Department of Transportation

In cooperation with
U.S. Department of Transportation
Federal Highway Administration

March 2025

The contents of this report reflect the views of the authors, who are responsible for the facts and accuracy of the data presented herein. The contents do not necessarily reflect the official views or policies of the Georgia Department of Transportation or the Federal Highway Administration. This report does not constitute a standard, specification, or regulation.

SI* (MODERN METRIC) CONVERSION FACTORS				
APPROXIMATE CONVERSIONS TO SI UNITS				
Symbol	When You Know	Multiply By	To Find	Symbol
LENGTH				
in	inches	25.4	millimeters	mm
ft	feet	0.305	meters	m
yd	yards	0.914	meters	m
mi	miles	1.61	kilometers	km
AREA				
in ²	square inches	645.2	square millimeters	mm ²
ft ²	square feet	0.093	square meters	m ²
yd ²	square yard	0.836	square meters	m ²
ac	acres	0.405	hectares	ha
mi ²	square miles	2.59	square kilometers	km ²
VOLUME				
fl oz	fluid ounces	29.57	milliliters	mL
gal	gallons	3.785	liters	L
ft ³	cubic feet	0.028	cubic meters	m ³
yd ³	cubic yards	0.765	cubic meters	m ³
NOTE: volumes greater than 1000 L shall be shown in m ³				
MASS				
oz	ounces	28.35	grams	g
lb	pounds	0.454	kilograms	kg
T	short tons (2000 lb)	0.907	megagrams (or "metric ton")	Mg (or "t")
TEMPERATURE (exact degrees)				
°F	Fahrenheit	5 (F-32)/9 or (F-32)/1.8	Celsius	°C
ILLUMINATION				
fc	foot-candles	10.76	lux	lx
fl	foot-Lamberts	3.426	candela/m ²	cd/m ²
FORCE and PRESSURE or STRESS				
lbf	poundforce	4.45	newtons	N
lbf/in ²	poundforce per square inch	6.89	kilopascals	kPa
APPROXIMATE CONVERSIONS FROM SI UNITS				
Symbol	When You Know	Multiply By	To Find	Symbol
LENGTH				
mm	millimeters	0.039	inches	in
m	meters	3.28	feet	ft
m	meters	1.09	yards	yd
km	kilometers	0.621	miles	mi
AREA				
mm ²	square millimeters	0.0016	square inches	in ²
m ²	square meters	10.764	square feet	ft ²
m ²	square meters	1.195	square yards	yd ²
ha	hectares	2.47	acres	ac
km ²	square kilometers	0.386	square miles	mi ²
VOLUME				
mL	milliliters	0.034	fluid ounces	fl oz
L	liters	0.264	gallons	gal
m ³	cubic meters	35.314	cubic feet	ft ³
m ³	cubic meters	1.307	cubic yards	yd ³
MASS				
g	grams	0.035	ounces	oz
kg	kilograms	2.202	pounds	lb
Mg (or "t")	megagrams (or "metric ton")	1.103	short tons (2000 lb)	T
TEMPERATURE (exact degrees)				
°C	Celsius	1.8C+32	Fahrenheit	°F
ILLUMINATION				
lx	lux	0.0929	foot-candles	fc
cd/m ²	candela/m ²	0.2919	foot-Lamberts	fl
FORCE and PRESSURE or STRESS				
N	newtons	0.225	poundforce	lbf
kPa	kilopascals	0.145	poundforce per square inch	lbf/in ²

* SI is the symbol for the International System of Units. Appropriate rounding should be made to comply with Section 4 of ASTM E380.
(Revised March 2003)

TABLE OF CONTENTS

EXECUTIVE SUMMARY	1
CHAPTER 1. INTRODUCTION	3
OVERVIEW	3
FINAL REPORT STRUCTURE	5
CHAPTER 2. LITERATURE REVIEW	7
CHAPTER 3. INVESTIGATION 1 - RECHANNELIZATION.....	10
METHODOLOGY	11
RESULTS IN LAB	13
CHAPTER 4. INVESTIGATION 2 – IN-LINE RF HARDWARE.....	17
CHAPTER 5. INVESTIGATION 3 - SOFTWARE DEFINED RADIO FOR	
U-NII-4 ESTIMATION AND DETECTION	32
ESTIMATOR / DETECTOR DESIGN AND TESTING	32
GRAPHICAL INTERFACE AND USER KIT FOR USING SDR FOR	
U-NII-4 DETECTION AND ESTIMATION	37
CHAPTER 6. CONCLUSIONS AND RECOMENDATIONS	38
RECOMMENDATIONS	40
APPENDIX A. RESEARCH ARTIFACTS	41
APPENDIX B. U-NII-4 DETECTION AND ESTIMATION KIT USER	
MANUAL	42
PURPOSE	42
MATLAB GUI.....	42
ARDUINO CODE	45
RESULTS.....	47
APPENDIX C. IN-LINE RF HARDWARE BOM.....	50
ACKNOWLEDGMENTS.....	51
REFERENCES	52

LIST OF FIGURES

Figure 1. Chart. Unlicensed Wi-Fi 5 spectrum (in Red) that could interfere with 5.9GHz CV services (in Yellow).	4
Figure 2. Photos. Screenshots from RP 22-18 showing low-cost aged U-NII-4 devices can show large out-of-band-emissions, which degrade DSRC communications. It is less likely that U-NII-5 (Wi-Fi 6E) transmissions will disrupt CV operations in C-V2X.	4
Figure 3. Photos. (left) DSRC OBU, (middle) the OwlBox open-source project used as U-NII-4 interferer, (right) DSRC RSU.....	12
Figure 4. Graphs. Compound figure showing results of increasing U-NII-4 guard band spacing by 5MHz until interference is of no-effect.	16
Figure 5. Photos. Collection of figures showing the design process of hairpin filters.....	19
Figure 6. Photo. Example fabricated printed circuit board filter for evaluation.	19
Figure 7. Photo. Frequency response of a sample fabricated RF filter. Ideally, the slopes would be drastic, but only about 3dB difference was obtained within the desired frequency range.....	20
Figure 8. Photo. Sample HPC script used to search for the optimal RF filter configuration.	22
Figure 9. Graph. In-lab results using various attenuators among 25 interferers. A 20dB attenuator provided 123% improvement in PRR, compared to without.....	23
Figure 10. Photos. On campus field tests with a 20dB attenuator and 25 interferers to observe V2I and I2V range.	24
Figure 11. Graphs. On campus field tests results with a 20dB attenuator and 25 interferers.....	25
Figure 12. Photo. 20dB attenuator + two circulators used in on campus experiments.	26
Figure 13. Graphs. On campus field tests results with a 20dB attenuator + two circulators in configuration to increase the I2V range by passing the attenuator for I2V signals among 25 interferers.....	26
Figure 14. Photos. Collection of photos from the first field tests on 10/21/2024 at Grant and Memorial with the attenuator + circulators in-line RF hardware treatment.	28
Figure 15. Graphs. 10/21/2024 Field tests at Grant and Memorial with the attenuator + circulators in-line RF hardware treatment did not capture the effects of the U-NII-4 interferers.	28
Figure 16. Photo. The U-NII-4 interferers closer to the RSU for the 2nd round of field tests conducted on 11/4/2024.	29
Figure 17. Graphs. V2I field re-test results from 11/4/2024. Without RF hardware treatment (left), and with RF hardware treatment (right).	30
Figure 18. Graphs. I2V field re-test results from 11/4/2024. Without RF hardware treatment (left), and with RF hardware treatment (right).	30

Figure 19. Photos. Custom enclosures developed for the RF hardware treatment.	31
Figure 20. Graph. ACPR data as an interference estimation is too noisy.	33
Figure 21. Photo. Final flowchart for detecting and estimating U-NII-4 interference activity in U-NII-4 Channel 177.	34
Figure 22. Photo. Determining the noise threshold for the estimator flowchart for the SDR used in this study.	35
Figure 23. Photo. The estimator performs well in a lab environment to detect the number of U-NII-4 interferers.	36
Figure 24. Graphs. Comparison of V2I PRR for previous project findings (left) and current project mitigation technique (right)	39
Figure 25. Graphs. Comparison of I2V PRR for previous project findings (left) and current project mitigation technique (right)	39
Figure 26. Photo. Version 0.2 of estimator software.....	43
Figure 27. Photo. Version 0.6 with GPS working.....	44
Figure 28. Photo. Version 0.6 showing data screen.	45
Figure 29. Photo. Version 1.0 main screen	48
Figure 30. Photo. Version 1.0 data screen.....	49
Figure 31. Photo. Assemble according to this configuration in a 3D printed case.	50

LIST OF ACRONYMS

CV = Connected Vehicle

DSRC = Dedicated Short-Range Communications (IEEE 802.11p)

LTE-V2X = Long Term Evolution Vehicle to Everything Communications

3GPP = Third Generation Partnership Project

C-V2X = Cellular Vehicle to Everything Communications (3GPP Rel 14 Sidelink)

BSM = Basic Safety Message

SPAT = Signal Phase and Timing Message

MAP = MapData Messages

SRM = Signal Request Message

SSM = Signal Status Message

TIM = Traveler information Message

U-NII-4 = Unlicensed National Information Infrastructure Region 4

GHz = Giga Hertz

MHz = Mega Hertz

ACP = Adjacent Channel Power

ACPR = Adjacent Channel Power Ratio

OOBE = Out of Band Emissions

V2I = Vehicle to Infrastructure

I2V = Infrastructure to Vehicle

PRR = Packet Reception Rate

EXECUTIVE SUMMARY

As a follow up to GDOT RP 22-18 where the research team discovered and reported the effect of real-world aged low-cost Wi-Fi 5 devices on connected vehicle (CV) roadside units (RSU), the work presented in this report for GDOT RP 23-16 explores various techniques to mitigate / detect interference from Wi-Fi 5 devices.

We conducted three major investigations seeking to answer these specific questions:

Investigation 1: What guard band size between Wi-Fi 5 devices and Vehicle-to-Everything (V2X) communications is necessary to reduce the effect of Wi-Fi 5 interference?

Our Recommendation: A guard band of at least 15MHz is necessary to adequately remove the harmful effects of Wi-Fi 5 devices. To implement these findings:

- Wi-Fi 5 devices operated by GDOT should **not** use: U-NII-4 Ch. 177, Ch. 175, Ch. 171, Ch. 163
- Wi-Fi 5 devices not operated by GDOT and within 300m of RSUs should be requested to **not** use: U-NII-4 Ch. 177, Ch. 175, Ch. 171, Ch. 163

Investigation 2: In what ways can an in-line radio frequency (RF) mitigation technique reduce the amount of Wi-Fi 5 interference?

Our Recommendation: An attenuator and two circulators are sufficient to reduce Wi-Fi 5 interference. To implement these findings:

- GDOT can purchase and assemble the components identified in this report for each RSU antenna, and can print the accompanying enclosure in 3D, and weatherproof the enclosure.

Investigation 3: How can software defined radio technology be used to detect Wi-Fi 5 interference?

Our Recommendation: High performance software defined radio technology can be used with an antenna assembly and MATLAB & SIMULINK to reliably detect Wi-Fi 5 interference (among other interference). To implement these findings: The research team provides an interference detection kit complete with hardware and software that GDOT can use to locate interference, without needing to hire a third-party firm to locate and identify interference.

CHAPTER 1. INTRODUCTION

OVERVIEW

The Georgia Department of Transportation (GDOT) and Kennesaw State University (KSU) via RP 22-28 completed a real-world interference study with actual device saturations both within the 30MHz licensed 5.9GHz spectrum and adjacent unlicensed bands to understand through real-world implementation how the existing 30MHz bandwidth can support CV application availability^[1]. Recommendations were provided, for which the work presented in this report implement those identified recommendations for various interference mitigation / detection strategies, specifically:

- Rechannelization (i.e., guard band spacing)
- In-line radio frequency hardware
- Software defined radio equipment

CV technologies will transform the way Georgians travel by providing safety, mobility, and environmental benefits. CV deployments in Georgia currently feature Roadside Unit (RSU) radios and a very small number of vehicle On-Board Unit (OBU) radios. The RSUs operate in 30MHz of licensed bandwidth known as the 5.9GHz Safety Band. That 30MHz of spectrum allotment is critical for enabling CV applications to provide the expected benefits. However, that vital band of spectrum resides next to unlicensed Wi-Fi 5 bands, which could cause adjacent channel interference and significantly degrade the CV applications' performance. As seen in figure 1, the channels which could affect CV application fidelity are: Ch. 173, Ch. 177, Ch. 175, Ch. 171, Ch. 163.

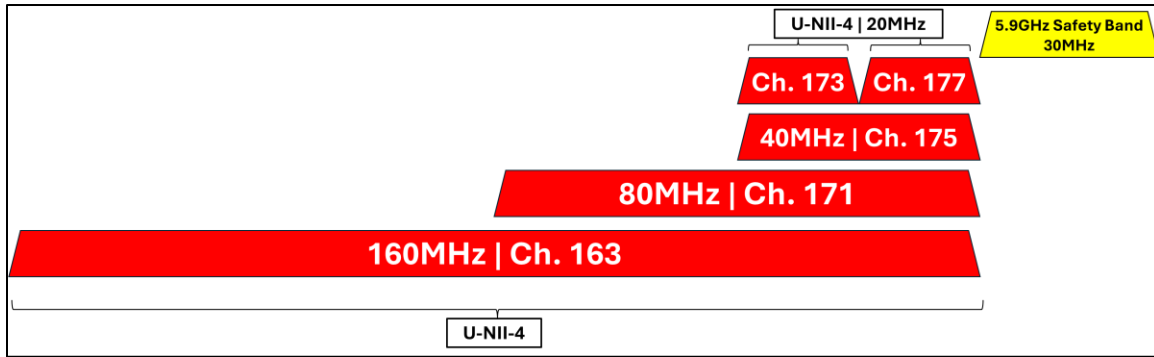


Figure 1. Chart. Unlicensed Wi-Fi 5 spectrum (in Red) that could interfere with 5.9GHz CV services (in Yellow).

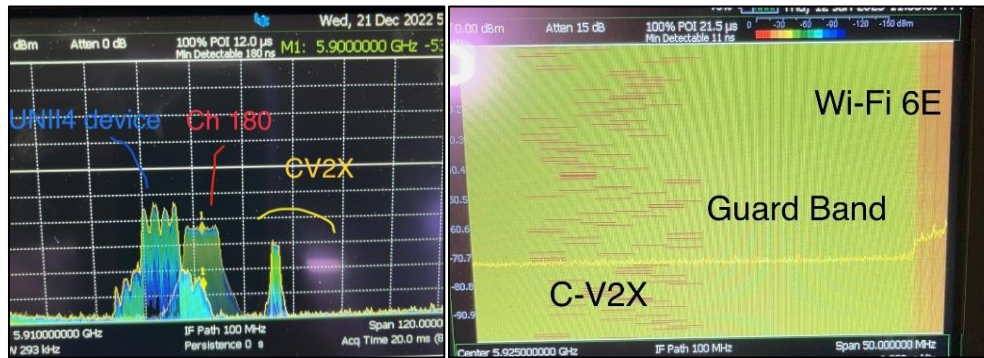


Figure 2. Photos. Screenshots from RP 22-18 showing low-cost aged U-NII-4 devices can show large out-of-band-emissions, which degrade DSRC communications. It is less likely that U-NII-5 (Wi-Fi 6E) transmissions will disrupt CV operations in C-V2X.

As seen in figure 2, unlicensed low-cost aged Wi-Fi 5 devices (known as Unlicensed National Information Infrastructure range 4, or U-NII-4 for short), can create out of band emissions which can worsen as the number of U-NII-4 devices increases. With the recent adoption of the Federal Communications Commission (FCC) Second Report and Order regarding the 5.9GHz band, Dedicated Short Range Communications (DSRC) is expected to be sunset in the United States within two years of the adoption, and cellular vehicle-to-everything communications (C-V2X) will be given full access to the 30MHz 5.9GHz Safety Spectrum ^[2]. From a previous report in GDOT RP 22-18, the research team

identified that DSRC is more susceptible to U-NII-4 interference (specifically in the Vehicle-to-Infrastructure links), and potentially C-V2X could experience similar U-NII-4 interference, though C-V2X was not observed either in lab or field settings to be affected by U-NII-4 interference up to 25 devices. In this new work, the research team decided to assess the performance of the mitigation techniques for DSRC RSUs (even though DSRC will be sunset), because the research team reasoned that if the techniques are successful (which they are) for DSRC they will with high likelihood be successful for C-V2X.

Though the research team is still unsure of the underlying reasons why DSRC is susceptible to U-NII-4 interference, the research team concluded from GDOT RP 22-18 that C-V2X is less susceptible because C-V2X semi-persistent scheduling (SPS) selects sub-channels within the 30MHz spectrum that have experienced less energy. Though even when C-V2X is forced to communicate near the U-NII-4 interference channel, the data in C-V2X signals reliably makes it through (at least up to 25 interferers and a mixture of 12 C-V2X on-board units (OBUs) and 4 RSUs). DSRC on the other hand does not avoid interference, thus U-NII-4 interference causes packet loss.

FINAL REPORT STRUCTURE

The structure of this report describes the three investigations conducted. Chapter 2 provides a literature review covering interference reports on CV equipment. Chapter 3 describes the rechannelization investigation and a brief recap of the equipment used in the study. Chapter 4 describes the suggested RF in-line hardware mitigation and reviews the development process in-lab, experimentation methodology, and field test results. Chapter 5 describes software defined radio investigation and the equipment used. Chapter 6 summarizes the

research findings and offers recommendations for implementation. The appendix and references are found at the end of this report.

CHAPTER 2. LITERATURE REVIEW

In the United States, the Safety Spectrum is between 5895-5925MHz. The FCC has revised the use of the 5.9 GHz band, initially allocated for Intelligent Transportation Systems (ITS) in 1999^[3]. The updated policy reserves the 5.895-5.925 GHz range exclusively for ITS to enhance traffic safety, while opening the remaining portion of the band to Wi-Fi to meet increasing demand and improve internet reliability. The retained ITS spectrum supports vehicle-to-vehicle and vehicle-to-infrastructure communications, essential for road safety and traffic management. This decision balances the need for robust traffic safety systems with growing demand for wireless connectivity. Additionally, aligning the 30 MHz reserved for ITS with international standards helps standardize technologies, reduce costs, and prepares for future advancements in traffic safety communication^[4].

Obscure Technologies Operating in the V2X Band: The US accommodates lesser-known uses of the V2X spectrum which can lead to in-band interference. The 5895-5925 MHz band allocated for V2X communication overlaps with complex regulations, including use by the **non-Federal Fixed-Satellite Service (FSS)** for Earth-to-space communication within the 5850-5925 MHz range^[5]. Additionally, the broader 5650-5925 MHz band is approved for military **Radio Location Service**, which uses radio waves to determine the position, speed, or characteristics of objects. This includes technologies like radar, applied in navigation, air traffic control, and maritime tracking^[6].

Technologies in Adjacent Bands that Can Cause Interference on V2X: The FCC has reallocated the lower 45 MHz of the 5.9 GHz band (5850-5895 MHz) for unlicensed use, such as Wi-Fi 5. This allows wireless communications like Wi-Fi networks to operate without a license, with indoor usage subject to specific power and technical limits to avoid

interference with nearby frequencies. The upper portion of this band is increasingly being used for **Wi-Fi 6E**, which extends Wi-Fi into the 6 GHz range. Additionally, the FCC has opened the lower 6 GHz band (5925-6425 MHz) for unlicensed use, supporting more advanced Wi-Fi applications indoors and outdoors. The 6425-7125 MHz range is also being explored for future unlicensed use and other broadband services^[7, 8, 9].

A literature search using TRB's TRID and Research in Progress (RiP) database shows that research centers are conducting research studies to understand interference issues on CV applications. Carnegie Mellon University recently completed a study that used extensive simulations to identify and assess alternative ways to meet the spectrum needs of CVs in a reduced 30MHz bandwidth, while also providing spectrum for Wi-Fi^[10]. The researchers were re-funded to develop additional simulations to understand other spectrum options amid interference^[11]. WSP USA was contracted to study the impacts of 5.9GHz spectrum changes on CV applications^[12]. A final report is being prepared, however, a white paper from the study reported that the impact of real-world saturation interference has not yet been tested, evaluated, or resolved^[13]. A literature search not using TRB's TRID and RiP databases, shows a press release and technical reports of on-going interference testing. These studies are only considering simulation or developing models from small empirical data to project the effects at scale. The Tampa Hillsborough Expressway Authority (THEA) is undertaking interference testing for the 5.9GHz Safety Band to identify the effects of unlicensed wi-fi signals. The researchers are installing a signal generator at a single location to test the effect of unlicensed interference on real-time CV applications like red-light violation warnings^[14]. The US DOT studies and continues to release technical reports on interference^[15, 16] and CAMP LLC testing has also conducted interference testing^[17],

however, studies to date do not consider saturation of real-world interference devices. The US DOT also recently released information related to an LTE-V2X congestion study amid a single interference point ^[18]. In addition, with the adoption of the second report and order by the FCC, there will be other questions about how outdoor transmissions (higher than the transmission used in this study) will affect C-V2X, if any at all.

CHAPTER 3. INVESTIGATION 1 - RECHANNELIZATION

As intelligent transportation systems (ITS) continue to advance and reliance on vehicular communication networks grows, maintaining reliable communication for all users has become a top priority. Dedicated Short-Range Communications (DSRC) were a foundational element of the CV ecosystem, facilitating crucial interactions between infrastructure and vehicles (I2V) as well as vehicles and infrastructure (V2I) - collectively known as Vehicle-to-Everything (V2X) communications. However, rising congestion within the U-NII-4 spectrum introduces the risk of interference from neighboring channels, which could compromise the system's reliability and performance. Even as the U.S. transitions to Cellular Vehicle-to-Everything (C-V2X) as the primary standard, potential interference from the U-NII-4 band may still pose a challenge. This is due to the interference that can occur when older U-NII-4 devices degrade and their emissions start to bleed into other channels, causing adjacent channel interference (ACI). ACI occurs when signals from one channel spill over into adjacent channels, leading to cross-channel noise and potential data loss.

ACI is a serious problem when it occurs in the DSRC band, since DSRC communication operates in the 5.9 GHz spectrum which was allocated for ITS applications. A potential solution for this issue is to increase the guard band size between the DSRC band and the U-NII-4 devices. Guard bands are unused portions of the spectrum that serve as buffers to prevent overlapping between signals in neighboring channels. By expanding these guard bands, in theory, interference could be significantly reduced, thereby enhancing the overall performance of devices in the DSRC band.

This solution proposed would investigate the functionality of increasing the guard band size for DSRC communication to see if it could be used to decrease interference in the DSRC 5.9GHZ safety band. Using real-world DSRC devices and lab analysis, the research team explored the impact of various guard band configurations on DSRC communication quality. The findings for this solution could be used to pave the way for other strategies that can be used to decrease interference.

METHODOLOGY

To test this method of interference mitigation, multiple different types of devices were needed. This included OBUs and RSUs and multiple low-cost U-NII-4 devices used to cause the interference. Specifically, as seen in figure 3:

- 1x Cohda Wireless DSRC OBU
- 1x Cohda Wireless DSRC RSU
- 2x Cohda Wireless RSU Antenna
- 1x Mobile Mark OBU Antenna (DSRC)
- 50x OwlBox Kit with (Low-Cost Aged U-NII-4 Interferers)

The OBU and the RSU devices were controlled using command line commands on a host computer. These command lines enabled the OBU and the RSU to send dummy packets to one another. The number of packets received by either device was then compared to the number of packets received by the other device. Two modes of communication were tested. The first mode was V2I communication. This was done by using the OBU and having it send dummy packets to RSU. The size of the packet payload was determined to be 362 bytes. This was determined by looking at the average packet size for two critical messages generated by OBUs: Basic Safety Messages (BSM) and Signal

Request Messages (SRM). The second mode of communication used in the study was I2V communication. As opposed to the OBU sending the packets to the RSU, the RSU sent dummy packets to the OBU. The packet size for RSU transmission was made to be 468 bytes. This was determined by looking at the average packet size for critical messages generated by RSUs: MAP, Signal Phase and Timing (SPAT), Traveler Information Message (TIM), and Signal Status Message (SSM).

To emulate low-cost aged U-NII-4 interferers (i.e., emulate how U-NII-4 devices may operate 15-20 years in the future.), the approach uses low-cost older IEEE 802.11a chipsets. The existing FCC license enables us to use modified Linux kernels which enable the IEEE 802.11a chipsets to broadcast ad hoc with IEEE 802.11p settings in U-NII-4 Ch. 177 at 20MHz. The interferers were the same devices used in GDOT RP 22-18 (1), composed of a raspberry pi compute module 4 connected to a daughter card with a radio chip, collectively called an OwlBox^[19]. The radio chip is connected to two antennas that allow the interferers to transmit to Ch. 177. These interferers were controlled using a python application run on a host computer. This application allowed the interferers to be controlled at the same time and change between transmitting at full rate and transmitting while emulating WLAN traffic.



Figure 3. Photos. (left) DSRC OBU, (middle) the OwlBox open-source project used as U-NII-4 interferer, (right) DSRC RSU.

RESULTS IN LAB

The study evaluated the impact of guard band size on DSRC communication quality by analyzing Packet Reception Rate (PRR) under varying interference conditions. Results were collected for both Vehicle-to-Infrastructure (V2I) and Infrastructure-to-Vehicle (I2V) communication modes, focusing on the number of packets successfully transmitted and received in each scenario. The U-NII-4 devices emulated WLAN traffic. Figure 4 shows the results of rechannelization where the x-axis is the number of U-NII-4 interferers from 0 to 45, in steps of 5, the y-axis is the packet reception rate from 0% to 100%. The plots show red lines (V2I) and blue (I2V) lines. It is desired to have both lines be above 80% PRR to ensure CV application reliability. A guard band of at least 15MHz or more between the U-NII-4 devices and the DSRC/C-V2X equipment is necessary to ensure CV application reliability. A guard band of at least 15MHz or more between the U-NII-4 devices and the DSRC/C-V2X equipment is necessary to remove the harmful effects of U-NII-4 emissions.

- **Baseline Performance:**
 - Without interference, the PRR for V2I communication averaged 100%, indicating reliable packet delivery when no adjacent channel noise was present. Similarly, I2V communication showed a baseline PRR of 100%, demonstrating high reliability in unimpeded conditions.
- **Impact of U-NII-4 Interference:**
 - As U-NII-4 interference was introduced, a noticeable decline in PRR was observed, with V2I dropping to 50% and I2V to 55% at maximum interference levels.

- **Effect of Guard Band Expansion:**

- Incrementally increasing the guard band size reduced interference and improved PRR in both communication modes. A guard band of 15 MHz led to large recovery in PRR (100% for V2I, 100% for I2V). The findings demonstrate that increasing the guard band size between DSRC and U-NII-4 channels effectively mitigates adjacent channel interference.

- **Interference Mitigation Potential:**

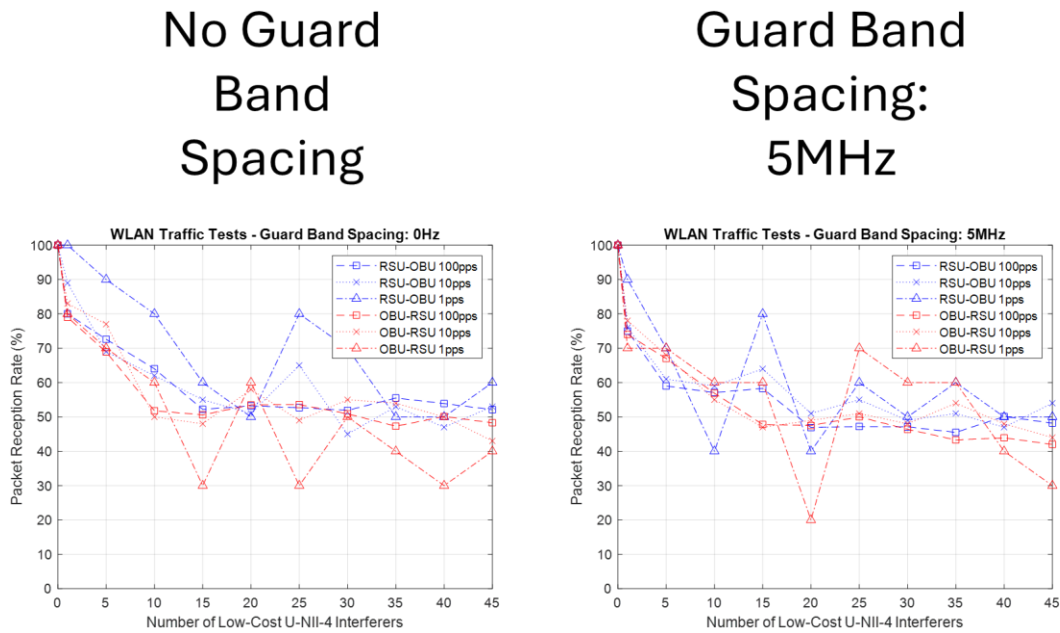
- Guard bands serve as a practical solution to reduce cross-channel noise, particularly in congested spectrum environments where U-NII-4 devices degrade over time.

- **Practical Implications:**

- Expanding the guard band enhances DSRC communication reliability, which is crucial for critical applications. Although this approach may reduce spectrum availability for other uses, the benefits to ITS reliability justify further exploration.

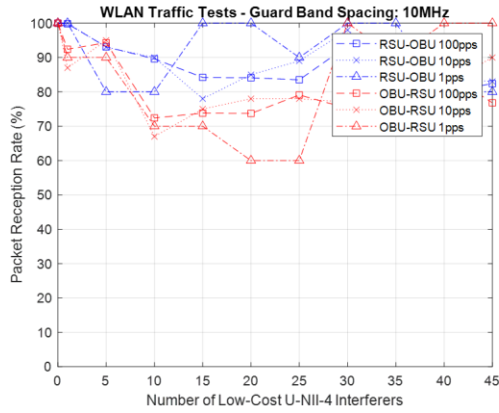
In summary, the study underscores the importance of addressing interference in DSRC communication and highlights guard band expansion as a viable strategy to improve V2X system performance. These findings contribute to ongoing efforts to optimize vehicular communication technologies and ensure their reliability in diverse operating conditions. If there are U-NII-4 devices operating around CV infrastructure, those U-NII-4 devices should be fixed to operate on Wi-Fi Channel 173 (that is exactly 20MHz separation). This will guarantee that CV infrastructure will remain unaffected. U-NII-4 devices near CV

equipment should not use: Ch. 177, Ch. 175, Ch. 171, Ch. 163. U-NII-4 devices near CV equipment should only use: Ch. 173. It is possible that GDOT and other stakeholders could petition the FCC to consider requiring U-NII-4 devices within 300m of CV infrastructure to automatically configure itself and its managed devices to only Ch. 173. This can be done through the U-NII-4 access points cross-referencing their GPS locations to a map of RSU installations. All client devices connected to the access point would only use Ch. 173. The U-NII-4 devices are indoor chipsets. The plots in figure 4 could change for outdoor U-NII-4 devices with higher power levels, however, there are no devices that can be procured to enable a realistic low-cost and aged outside U-NII-4 devices.

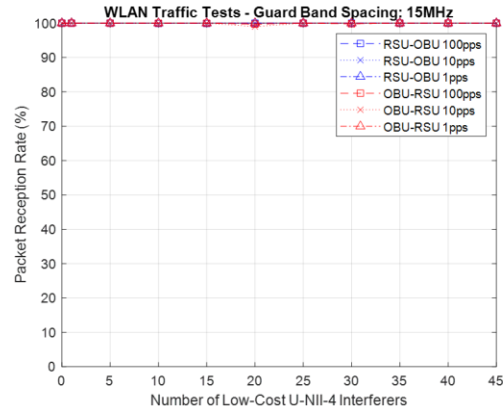


A. Subfigure of U-NII-4 interference with no guard band spacing (left) and 5MHz of guard band spacing (right).

Guard Band Spacing: 10MHz

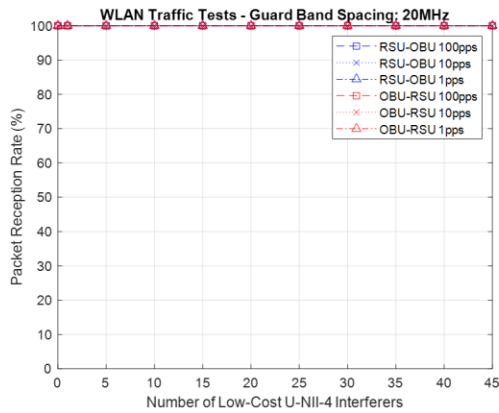


Guard Band Spacing: 15MHz

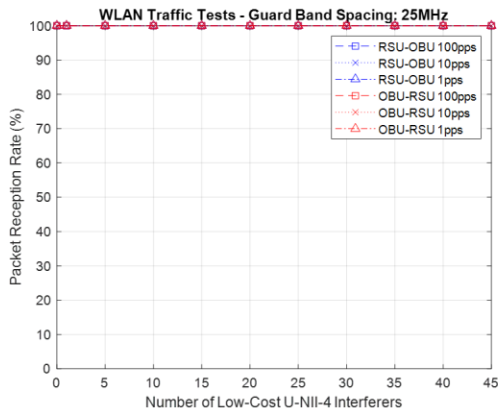


B. Subfigure of U-NII-4 interference with 10MHz of guard band spacing (left) and 15MHz of guard band spacing (right).

Guard Band Spacing: 20MHz



Guard Band Spacing: 25MHz



C. Subfigure of U-NII-4 interference with 20MHz of guard band spacing (left) and 25MHz of guard band spacing (right).

Figure 4. Graphs. Compound figure showing results of increasing U-NII-4 guard band spacing by 5MHz until interference is of no-effect.

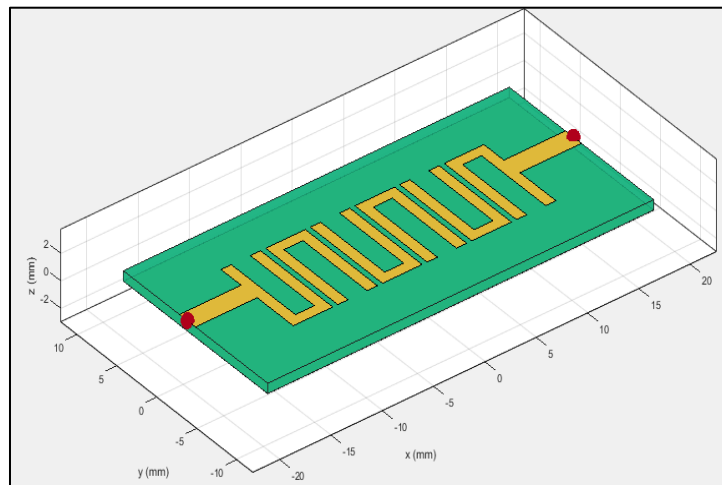
CHAPTER 4. INVESTIGATION 2 – IN-LINE RF HARDWARE

Beginning in June 2024, the research team began research on the development and function of varying RF filters, specifically within the MATLAB environment due to its accessibility and low barrier of entry. The research team found that MATLAB can generate and test filters of various specifications. With this development, these tools were used to design and create a solution for the problem of U-NII-4 interference with DSRC. The initial plan was to create a microstrip band pass filter, which had a rising edge around 5.895 GHz and a falling edge around 5.905 GHz, see figure 5 for a sample frequency response of the filter. This would allow for the full range of DSRC to be allowed in, while attenuating noise.

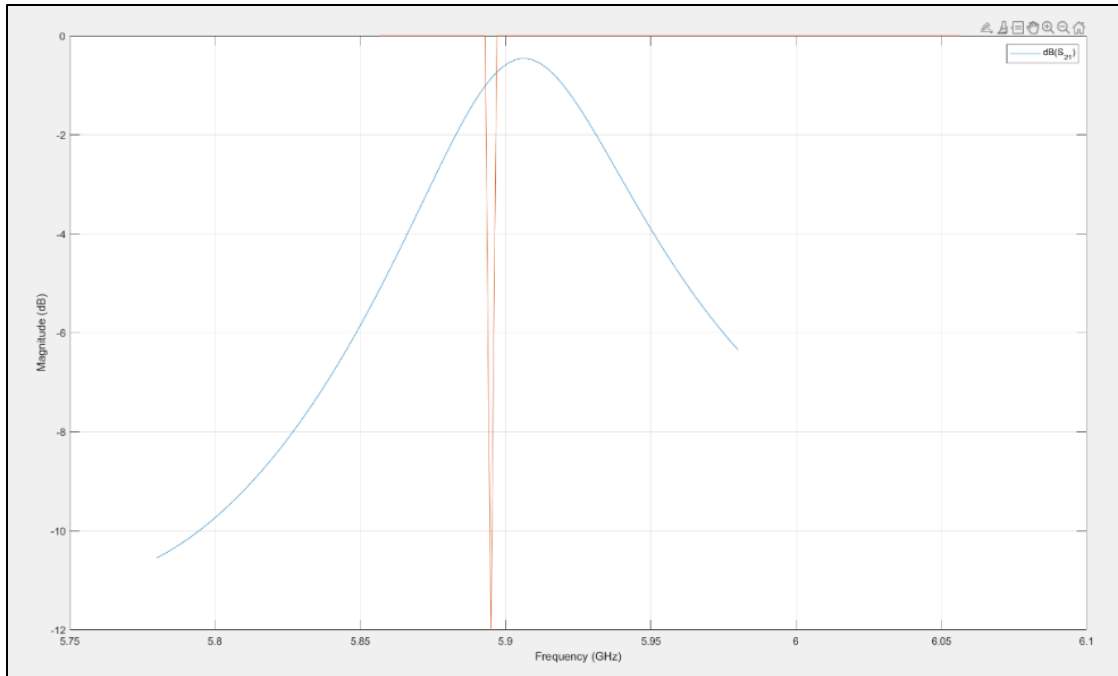
The first step of this process was to create a script to generate the filters and create the necessary Gerber files for printing the printed circuit boards (PCBs), as seen below in figure 5. With this completed, the next step began a process of trial and error to see how the different factors and variables of the code changed the results of the filter generation. In July 2024 the first iterations of filter designs were completed and the Gerber files sent off to a printed circuit board vendor for manufacturing. In the time of manufacturing and delivery testing of filters continued, as well as attenuators, which will be addressed later in this report. A generated 3D model of one of the generated filters can be found below in figure 6.

<pre> 1 %% GDOT RP 23-16 PCB Microstrip Hairpin RF Filter Test Script 2 clear % Clear workspace 3 clc % Clear command window 4 close all % Close all open figures 5 6 filter = filterHairpin; % Use Built-In MATLAB Hairpin Filter Object 7 filter.Height = 0.76e-3; % Height of substrate 8 filter.Substrate.EpsilonR = 2.54; % Dielectric constant (i.e., how compact 9 filter.FilterOrder = 6; % Number of resonant elements 10 filter = design(filter,6e9,'FBW',20,'RippleFactor',0.1); 11 % design, creates the filter. 12 % Centered on 6GHz, with a desired 20% fractional passband, 13 % with a .1 maximum allowable variation (in decibels) in the passband response 14 15 % Show the 3D Model of the PCB Filter 16 figure 17 show(filter) </pre>	
--	--

A. Subfigure of MATLAB code for designing a hairpin filter on printed circuit board (PCB).



B. Subfigure of rendering of a hairpin filter.



C. Subfigure of S21 simulation output in MATLAB of a hairpin filter.

Figure 5. Photos. Collection of figures showing the design process of hairpin filters.

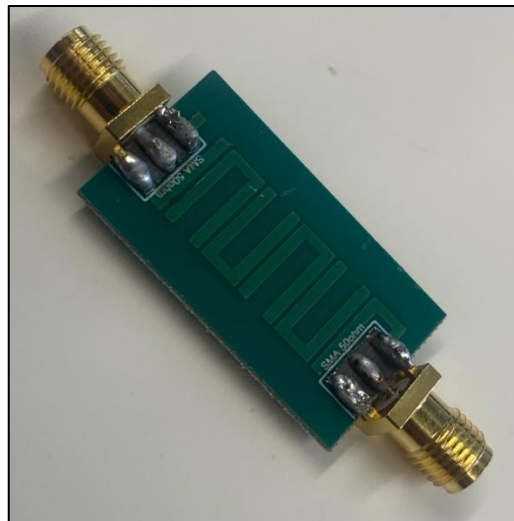


Figure 6. Photo. Example fabricated printed circuit board filter for evaluation.

Once delivered, SMA connectors were soldered to the pads of the PCB filters and began reading the S21 plots of the designs using a Network Analyzer (i.e., a Real-Time Spectrum Analyzer with Network Analyzer on loan from the vendor) to determine if the filter frequency response matches the simulation. These tests were rather disappointing, as the filters were not as refined as hoped, and a few did not work at all as they were missing the necessary pads, see figure 7.

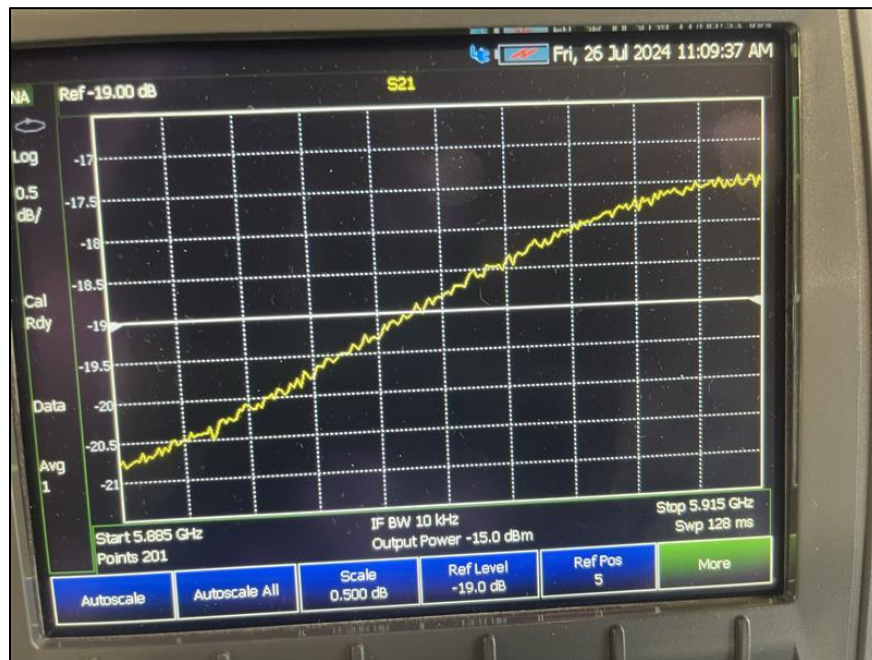


Figure 7. Photo. Frequency response of a sample fabricated RF filter. Ideally, the slopes would be drastic, but only about 3dB difference was obtained within the desired frequency range.

Although the results were not as strong as hoped, in-lab interference tests showed that the filters did help recover the PRR of both the I2V and V2I transmissions. At this point it was discovered that attenuation can be useful within certain scenarios and credited the improvement to the overall attenuation from the filter. Additional experiments were

performed by cascading multiple filters in simulation to increase the filter's Q (i.e., how narrow the passband is), and found that this would essentially increase the order of the filter. This allowed for steeper slopes for the S21 curves.

After a period of trial and error, and ultimately not finding the results desired, the research team began development of a MATLAB script to run on the Kennesaw State University Student High Performance Computing (HPC) cluster. This script would run over a set amount of time, testing 100,000 different filters by stepping through a set range of variables and testing for every combination possible. Once the script was developed, it was run on the HPC for a total of twenty days: passing its available time to run. With some adjustments, the total number of filters was lowered to 10,000 and split the total into four different scripts that simulated 2,500 filters each. The results showed that various filters had the same behaviors, but did have differing variables. The research team continues the research and development within this area, also utilizing a KSU ECE HPC server, but none of the filters created by this script have been fabricated. A version of the script can be found below in figure 8.

```

EpsilonR = 2.54;%Material conductivity, Don't change.
h = 0.76e-3;%Height of PCB, Don't change
Z0 = 50;
f = linspace(5.885e9,5.9e9,2);

load hpc_filter_ds1_10000.mat
q = p_ds1;
L=length(q);
bdy = zeros(1,length(q));
bslope = zeros(1,length(q));
parfor index = 1:length(q)
    iN = q(index,1); iC = q(index,2); iB = q(index,3); iR = q(index,4);
    try
        filter = filterHairpin;
        filter.Height = h;
        filter.Substrate.EpsilonR = EpsilonR;
        filter.FilterOrder = iN;
        filter = design(filter,iC,'FBW',iB,'RippleFactor',iR);
        spar = sparameters(filter, f, 1);
        y=mag2db(abs([spar.Parameters(2, 1, :)]));
        y1 = y(1);
        y2 = y(2);
        dy = y2 - y1;
        slope = (dy)/(15e6);
        bdy(index) = dy;
        bslope(index) = slope;
    catch
        continue
    end
    if mod(index,10)==0
        fprintf('Progress: %.2f%% (%d of %d)\n', (index/L)*100, index, L)
    end
end

BDY = 0;
BSLOPE = 0;
for k = 1: length(bdy)
    if (bdy(k) < BDY) && (bslope(k) < BSLOPE)
        BDY = bdy(k);
        BSLOPE = bslope(k);
        K = k;
    end
end
BDY
BSLOPE
format long
bestN = q(K,1)
bestCenterFreq=q(K,2)
bestRipple = q(K,3)
bestBandwidth = q(K,4)
q(K)

```

Figure 8. Photo. Sample HPC script used to search for the optimal RF filter configuration.

While waiting for the PCB filters to be delivered from the manufacturer, the research team decided to test how to run an attenuator in-line between the RSU and the antenna. In lab, the research team found that this helped both the V2I as well as I2V, even with 25 interferers on. This is possible because the RSU demodulation chain automatically

recovers V2I signals it needs via an equalization step in the demodulation, meaning attenuation quiets all frequencies including U-NII-4 and DSRC, leading to less interference, which the RSU radio equalizes the attenuation where the data carriers are.

Within a lab environment the research team connected attenuators in-line with the stock antennas and activated 25 interferers. The research team then ran ten trials for various attenuation levels, reading the PRR of V2I. After ten trials of the same attenuation level, the research team would then change attenuators until it was found that a 20dB attenuation level performed with 123% improvement compared to without the attenuation, see figure 9.

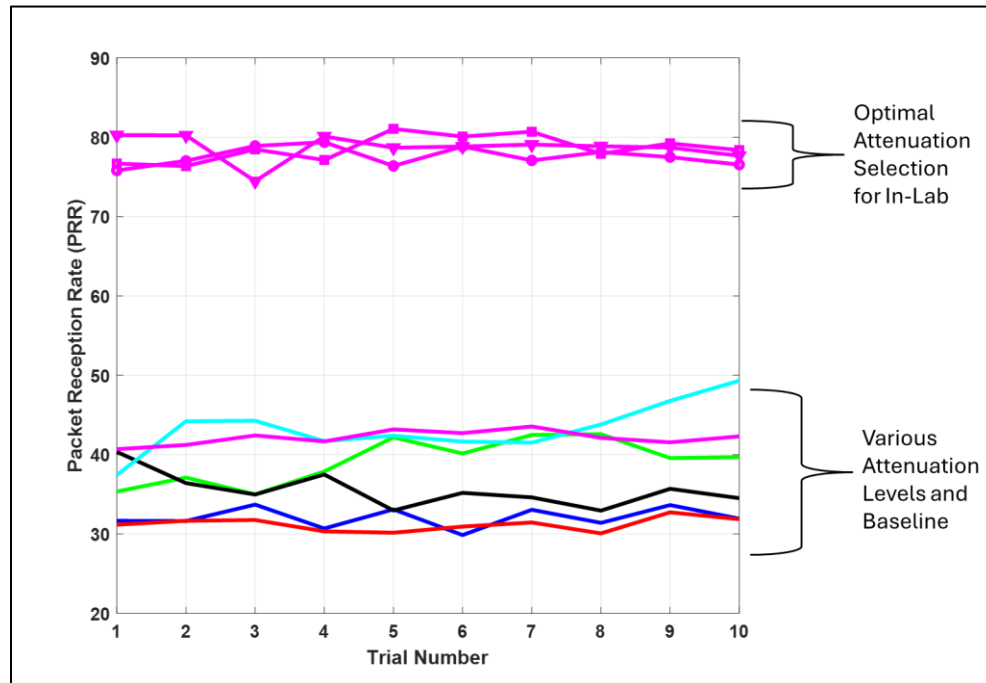


Figure 9. Graph. In-lab results using various attenuators among 25 interferers. A 20dB attenuator provided 123% improvement in PRR, compared to without.

However, it was assumed that this solution would lessen the effective range of the RSU, for both V2I and I2V. Running on campus field tests (seen in figure 10) proved this suspicion, with I2V being essentially unsalvageable beyond 20 meters, with a slight increase in performance when interference is present. However, it also demonstrated that when in the effective range, the PRR jumped from 50% to a nearly 100% PRR for V2I. The results of the tests are shown below in figure 11.

A 20 dB attenuator was configured in-line with the stock RSU antennas and proceeded to run a test sending a consistent number of packets. The distance between the RSU and OBU was varied by moving the vehicle containing the OBU closer or farther away. This test was performed with a fixed number of interferers on or off.



Figure 10. Photos. On campus field tests with a 20dB attenuator and 25 interferers to observe V2I and I2V range.



Figure 11. Graphs. On campus field tests results with a 20dB attenuator and 25 interferers.

In figure 11, I2V and V2I have a drastic drop in effective range, however the I2V sees a much sharper decline. As for the V2I, the PRR increased drastically between the two runs. A new goal was set to improve the I2V performance while the 20dB attenuator is in use. Using circulators, the in-line attenuation was bypassed and output a practically unaffected I2V signal. Building a new configuration, as seen below in figure 12, additional campus tests were performed and found that the configuration returned the I2V effectiveness to how it performed without the inline attenuation, see figure 13. However, V2I still saw a drastic decrease in effective range, which was not surprising given the previous tests. The methodology for the attenuator + circulator tests were similar as the previous tests with just

attenuator, with the only difference being a circulator solution with both 20 dB and 30 dB options.

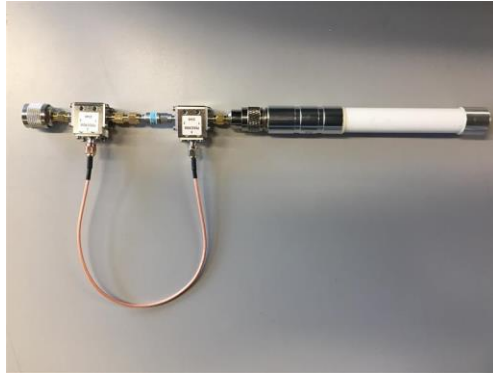


Figure 12. Photo. 20dB attenuator + two circulators used in on campus experiments.

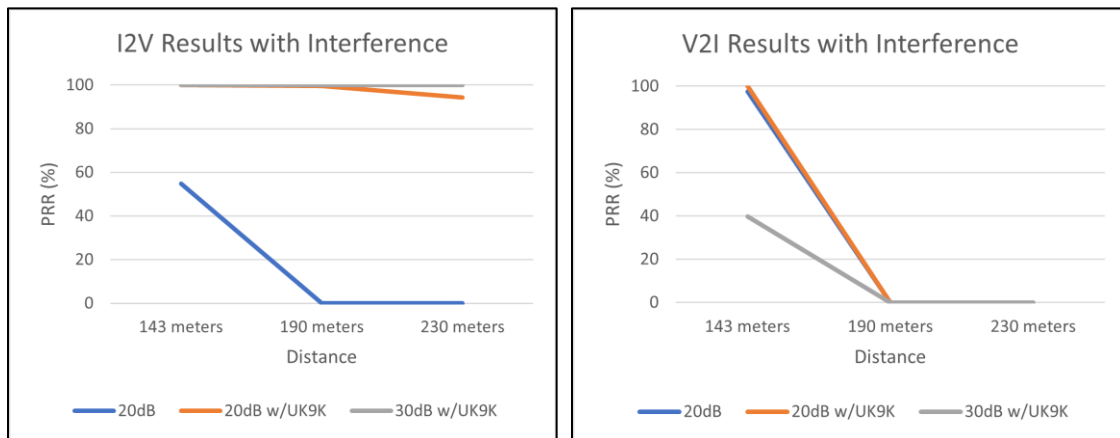


Figure 13. Graphs. On campus field tests results with a 20dB attenuator + two circulators in configuration to increase the I2V range by passing the attenuator for I2V signals among 25 interferers.

These results warranted in field testing to confirm the solution would be just as effective within a real-world environment. The first field test was performed on the 21st of October 2024. The results of this test showed the reception of BSMs decreased with the use of the attenuation solution, however the unattenuated runs also showed improvement

compared to the tests results from last year. After some in-lab tests from a different team, it was confirmed that there was a firmware update that improved the stock performance. These tests consisted of the use of a real, in service, RSU and an OBU in a controlled test vehicle. The field test was performed at Grant and Memorial where GDOT RP 22-18 tests were run, see figure 14. The two units were configured to send basic safety messages at the standard rate of 10 per second. During these tests a team of researchers were placed near the RSU, in control of U-NII-4 interferers. Another research team rode inside the test vehicle, who would pass by the RSU team on east-west approaches (the mainline) and communicate to them to increase activated interferers in increments of five. This process was repeated until reaching the max number of interferers, around 45 interferers.



A. Subfigure of U-NII-4 interferes on location.



B. Subfigure of in-line RF treatment installed in the field.



C. Subfigure of in-field vehicle used equipped with OBU.

Figure 14. Photos. Collection of photos from the first field tests on 10/21/2024 at Grant and Memorial with the attenuator + circulators in-line RF hardware treatment.

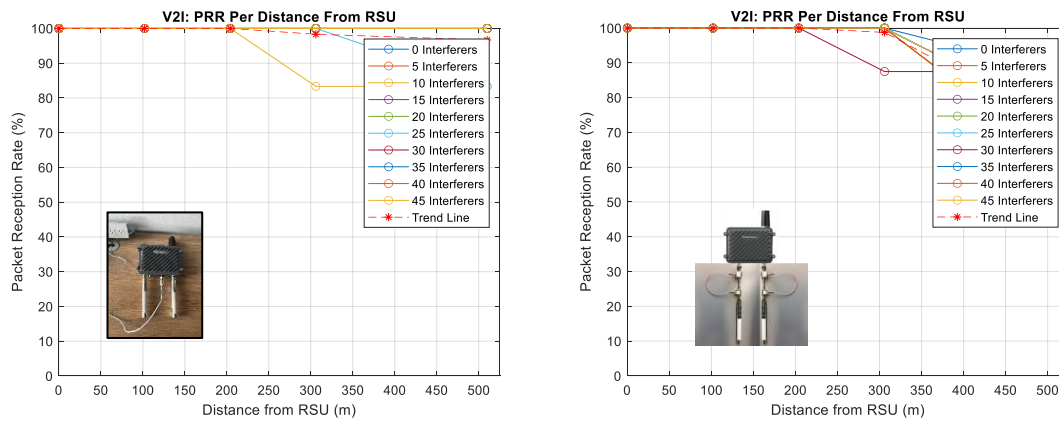


Figure 15. Graphs. 10/21/2024 Field tests at Grant and Memorial with the attenuator + circulators in-line RF hardware treatment did not capture the effects of the U-NII-4 interferers.

The results showed that the treatment did not disrupt V2I reception distance, see figure 15, an improvement from the on-campus tests (probably due to the increased height of the RSU). However, the effect of U-NII-4 interferers was not observed, see figure 15 again, because the interferers were set too far from the RSU. The research team is not sure if the

RSU, which was also tilted in a different orientation from GDOT 22-18 experiments, created a null in the RSU reception which just so happened to align with where the U-NII-4 interferers were.

With the results of previous tests, it was determined to run another field test in which the interferers were positioned closer to the RSU to confirm that the effect of the U-NII-4 interferers was observable without the in-line treatment, see figure 16.



Figure 16. Photo. The U-NII-4 interferers closer to the RSU for the 2nd round of field tests conducted on 11/4/2024.

The methodology of these re-tests was very similar to the last in-field tests; however, this time the research team increased the number of active interferers by increments of 10 to reduce total test time. The second test was performed on the 4th of November 2024. The results shown in figure 17 are excellent for V2I. It was found that the V2I had an overall increased performance, however, the I2V was still negatively impacted by the in-line

treatment, see figure 18. The research team is unsure at this time why the circulator solution did not perform as well as the original distance testing from 10/21/2024 field-tests.

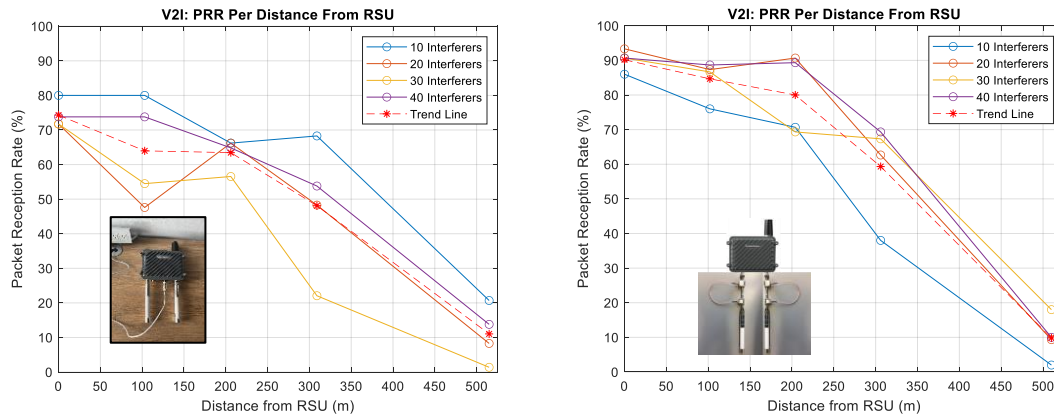


Figure 17. Graphs. V2I field re-test results from 11/4/2024. Without RF hardware treatment (left), and with RF hardware treatment (right).

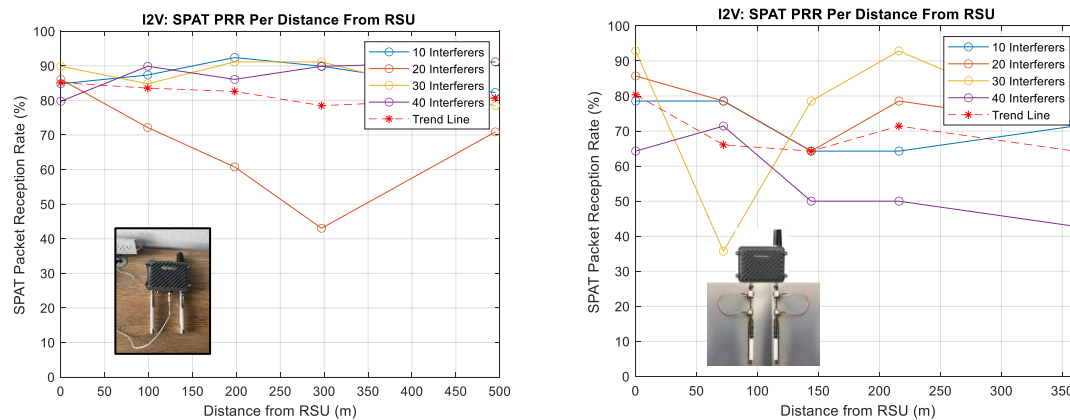


Figure 18. Graphs. I2V field re-test results from 11/4/2024. Without RF hardware treatment (left), and with RF hardware treatment (right).

To ensure the safety and functionality of the devices during field testing, custom enclosures were designed and fabricated for both the interferers and the attenuation + circulators solution, see figure 19. These enclosures were developed to securely house the components and protect them from environmental factors and physical damage. Utilizing 3D printing technology, created custom designs were created that provided precise fit and structural

integrity. This approach allowed for rapid prototyping and optimization to meet the specific requirements of the project. Please review the BOM in Appendix C for component details.

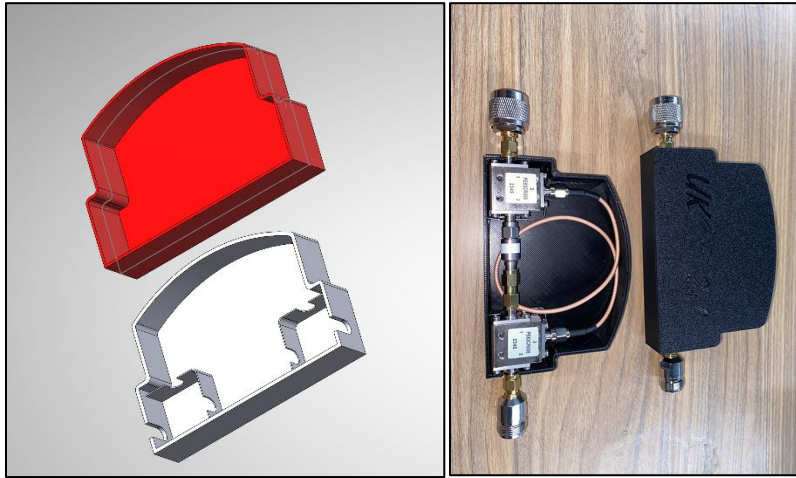


Figure 19. Photos. Custom enclosures developed for the RF hardware treatment.

CHAPTER 5. INVESTIGATION 3 - SOFTWARE DEFINED RADIO FOR U-NII-4 ESTIMATION AND DETECTION

The purpose of this investigation is to use an algorithm to analyze the raw signal data coming in through an SDR (software defined radio). Measuring the U-NII-4 band while focusing on the amount of power seeping through the spectrum mask into DSRC Ch. 180. It is important that the equipment measures U-NII-4 interference to understand how it affects the reliability of DSRC communications.

ESTIMATOR / DETECTOR DESIGN AND TESTING

The first approach was using ACPR (adjacent channel power ratio). It was believed that ACPR would give a good representation of the amount of power bleeding into the main channel. A couple of different ways of handling ACPR were experimented with. Initially experiments attempted to compute the ACPR by taking the adjacent channel (U-NII-4 Ch. 177) and dividing it by the RF power in the main channel (DSRC Ch. 180). Next this measurement was put into a matrix of varying sizes to find the moving average of that matrix. This approach had a couple fundamental flaws that were later improved upon in subsequent designs. Namely because it couldn't handle quick moving and dynamic changes to the incoming data stream from the SDR (i.e. it could find interference but wouldn't give an accurate representation of the amount of interference this is shown in figure 20).

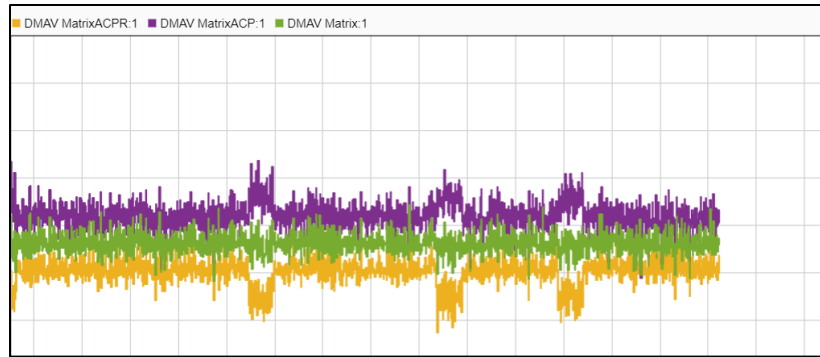


Figure 20. Graph. ACPR data as an interference estimation is too noisy.

Although it appears there is some kind of change in ACPR, it is spiking in the opposite direction of what might be expected. ACPR is extremely noisy, and it would be hard to programmatically quantify this data. For these reasons the research team transitioned from measuring the amount of interference to detecting the number of instances of U-NII-4 packets via a time scope. This was merely a test to make sure that each “sample batch” of interference could be seen. Using this knowledge, the equipment started to work directly with the raw data at a real-time rate. The research team first found the magnitude of the complex signals; this would serve to isolate the signal power from the raw data making it easier to quantify and analyze interference levels. The output would then go through a windowed integrator, which sums up the signal over a specified window. This would smooth out the signal power over time giving an average view of the interference levels. After integration, the absolute value of the signal is taken to ensure that the values won't be negative, this would be followed by squaring the signal further emphasizing higher power in the signal. Improving upon this base, the signal processing chain seen in figure 21 is the final stable and reliable flowchart.

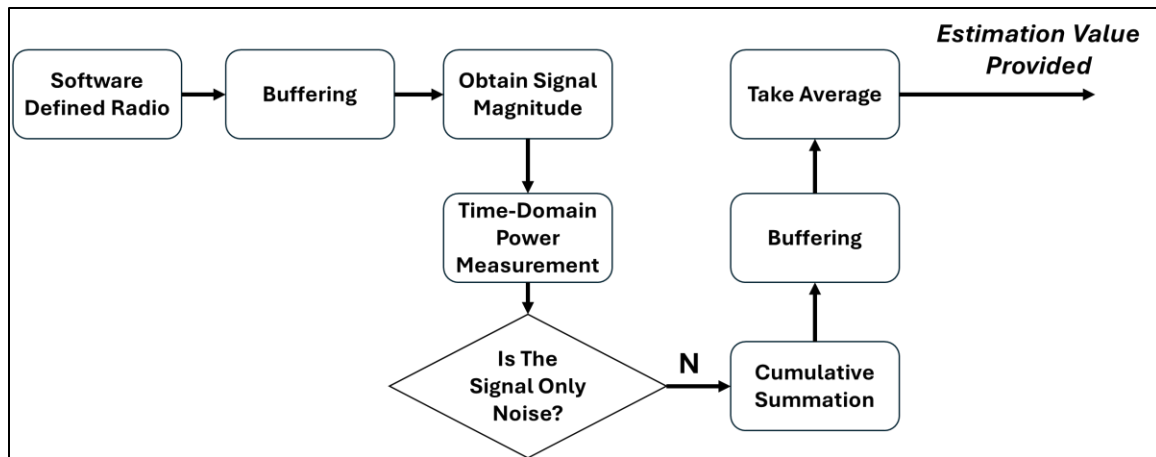


Figure 21. Photo. Final flowchart for detecting and estimating U-NII-4 interference activity in U-NII-4 Channel 177.

To begin this process, a collection of .04 seconds worth of data, which is 1 million samples, is placed in a buffer to allow for processing. After collecting the data which consist of real and imaginary numbers, the data stream is converted into a double data type by finding the magnitude squared of the set of all 1 million samples. From there the number is sorted if it meets the minimum value threshold for the SDR to be considered interference instead of noise, and then finally averaged. To determine if noise or the signal desired to be measured, the detector was calibrated by measuring a threshold for U-NII-4 interference when with no interferes never went above a certain empirical level as shown in figure 22. This ensured reliability in the estimator by reducing false positives.

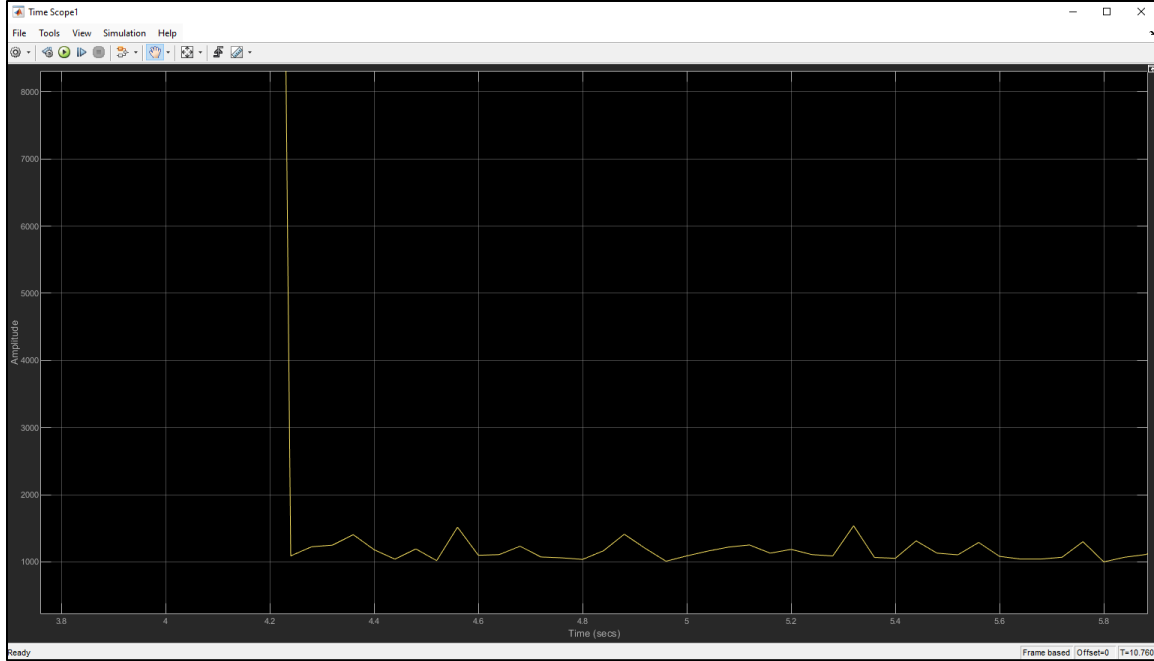


Figure 22. Photo. Determining the noise threshold for the estimator flowchart for the SDR used in this study.

This value was determined to be $t = 2.5 \times 10^3$. When the data is less than t it zeroes out.

When the data is above this value it is normalized using the equation $y = \frac{u}{\max(u)}$.

This normalization gives context to the result as it sets a max possible value at 1. With this the end value of the cumulative sum is computed. Importantly this end value will be bounded on a scale of 0 to 1 million, as the frame to be processed was set after the SDR to be 1 million samples. Finally, 12 of these end numbers are buffered and average to find the average power over the last half second. When in a lab setting, the estimator / detector was very stable, and could show the number of estimators during time of the experiments, see figure 23.

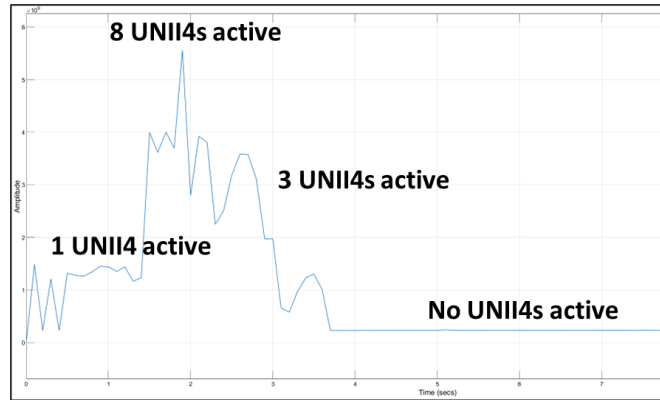


Figure 23. Photo. The estimator performs well in a lab environment to detect the number of U-NII-4 interferers.

The estimator was taken on a war drive near select midtown and downtown RSU locations (both planned and installed), supplied by GPS locations from GDOT. There was no significant interference, however, near the Georgia World Congress Center area, a burst of unidentified high-power interference was observed (could be communications or radar systems). It is intermittent so it is with low likelihood that this interference disrupts CV applications. The lab results shown in figure 23 demonstrate the effectiveness of the final approach of the estimator in detecting and quantifying interference in the U-NII-4 band. The lab data shown highlights the magnitude of interference, providing valuable insights into its behavior over time. Overall, the results confirm that the estimator is effective in detecting and quantifying interference in the U-NII-4 band. By leveraging real-time processing, normalization, and threshold-based detection, the system provides a robust framework for analyzing interference and its impact on CV communication.

GRAPHICAL INTERFACE AND USER KIT FOR USING SDR FOR U-NII-4 DETECTION AND ESTIMATION

The U-NII-4 detection / estimation kit comes complete with:

- Software Defined Radio (USRP X310)
- Antennas and Cabling
- A graphical user interface

The kit is supplied with a user manual featured as Appendix B.

CHAPTER 6. CONCLUSIONS AND RECOMENDATIONS

Through the course of the three investigations a wide array of techniques was employed to mitigate wireless interference. Rechannalization by introducing a virtual guard band near RSU locations is the most straightforward way to reduce the harmful effect of low-cost aged U-NII-4 devices. The RF in-line hardware configuration discovered through this project is just one mitigation technique that could be employed at the device level. The configuration discovered through this project is not completely transparent to the radio operations since the various hardware interfaces via the SMA connectors and the inline attenuator can reduce the performance of I2V and V2I. Compared to GDOT RP 22-18, this research project discovered and validated in the field an improvement to PRR for V2I with a tradeoff of distance, see figure 24. The I2V performance is reduced with the mitigation technique of this project, see figure 25. However, it is the opinion of the authors of this report that a well-engineered passive RF filter is still needed to provide the most low-cost option while not significantly degrading I2V or V2I performance. Lastly the discovery of the software defined radio signal processing chain is adequate for GDOT to use for any other interference studies on GDOT owned wireless equipment. However, the final kit could still be improved upon to be more reliable, there are times when running the kit that the SDR will need to be restarted.

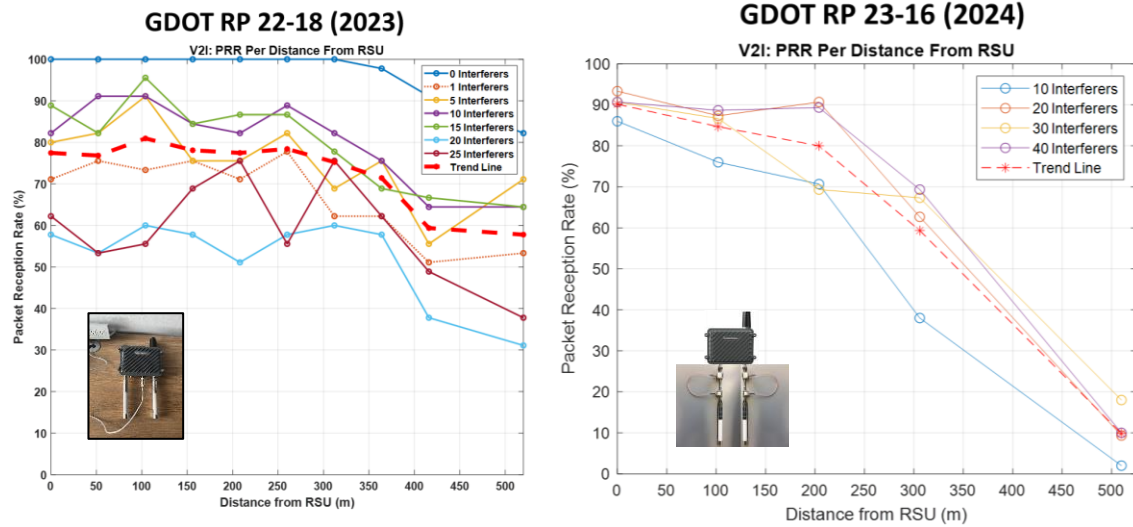


Figure 24. Graphs. Comparison of V2I PRR for previous project findings (left) and current project mitigation technique (right)

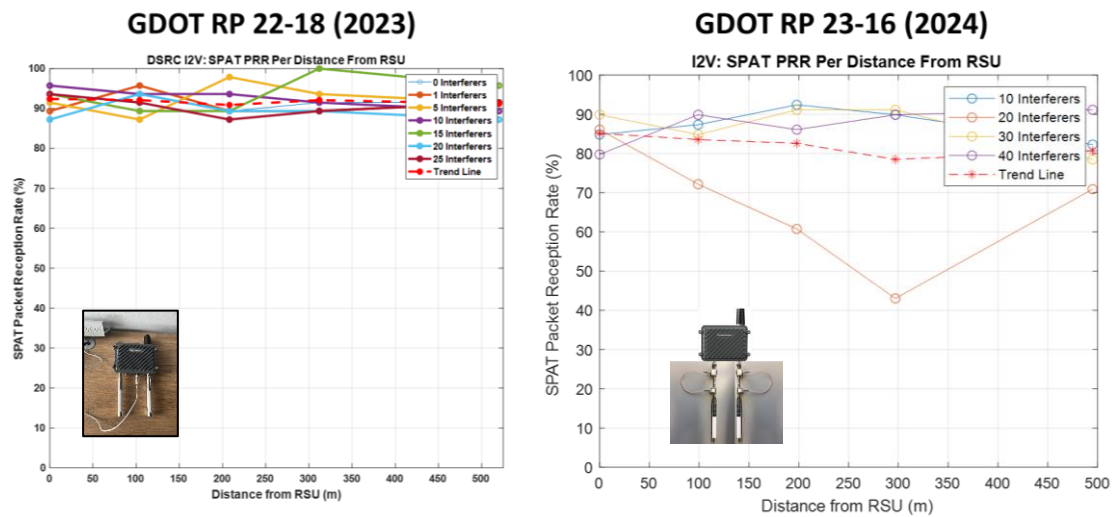


Figure 25. Graphs. Comparison of I2V PRR for previous project findings (left) and current project mitigation technique (right)

RECOMMENDATIONS

Recommendation 1: A guard band of at least 15MHz is necessary to adequately remove the harmful effects of Wi-Fi 5 devices. To implement these findings:

- Wi-Fi 5 devices operated by GDOT should **not** use: U-NII-4 Ch. 177, Ch. 175, Ch. 171, Ch. 163
- Wi-Fi 5 devices not operated by GDOT and within 300m of RSUs should be requested to **not** use: U-NII-4 Ch. 177, Ch. 175, Ch. 171, Ch. 163

Recommendation 2: An attenuator and two circulators are sufficient to reduce Wi-Fi 5 interference with noticeable impact to I2V and V2I performance. To implement these findings:

- GDOT can purchase and assemble the components identified in this report for each RSU antenna, and can print the accompanying enclosure in 3D, and weatherproof the enclosure.

Recommendation 3: High performance software defined radio technology can be used with an antenna assembly and MATLAB & SIMULINK to reliably detect Wi-Fi 5 interference (among other interference). To implement these findings: an interference detection kit is provided complete with hardware and software that GDOT can use to locate interference, without needing to hire a third-party firm to locate and identify interference. The current software version is not optimized and often requires a restart and is a solid foundation to build from now that the signal processing chain is discovered.

APPENDIX A. RESEARCH ARTIFACTS

All PCAP files can be made available upon request.

All multimedia can be made available upon request.

All WLAN Interference source code is available here: https://github.com/Intelligent-Mobile-Device-Lab-at-KSU/owlbox_files

Control Server Code in Python can be made available upon request.

MATLAB post-processing scripts can be made available upon request.

Please contact: bkihei@kennesaw.edu

APPENDIX B. U-NII-4 DETECTION AND ESTIMATION KIT USER MANUAL

PURPOSE

For capturing U-NII-4 activity, there are two types of antennas in use: the omnidirectional and the rotational antenna. Microcontroller code and MATLAB code for the manual antenna were created that would allow it to passively read incoming signals, update the user, and rotate the antenna in the desired direction via serial input from the user. The user will interface with the system through a MATLAB GUI that sends and receives serial input from an Arduino Mega wired to an IR sensor and a NEMA 17 Stepper Motor that actuates the rotation of the antenna.

MATLAB GUI

The prototype started off as most GUI applications do, a blank screen. Changes to the GUI were small additions slowly building up functionality of the prototype. Simple features were added to the app first such as lamps on the screen to show if a particular system was not working properly. However, they were all easy to implement in MATLAB. One major obstacle for the app was how MATLAB does not support full multi-threading. There were a lot of components that needed to be working simultaneously, sometime unreliable. The solution was an update function using the Timer object, this allowed the app to automatically run through a list of updates for each component about every 1 second.

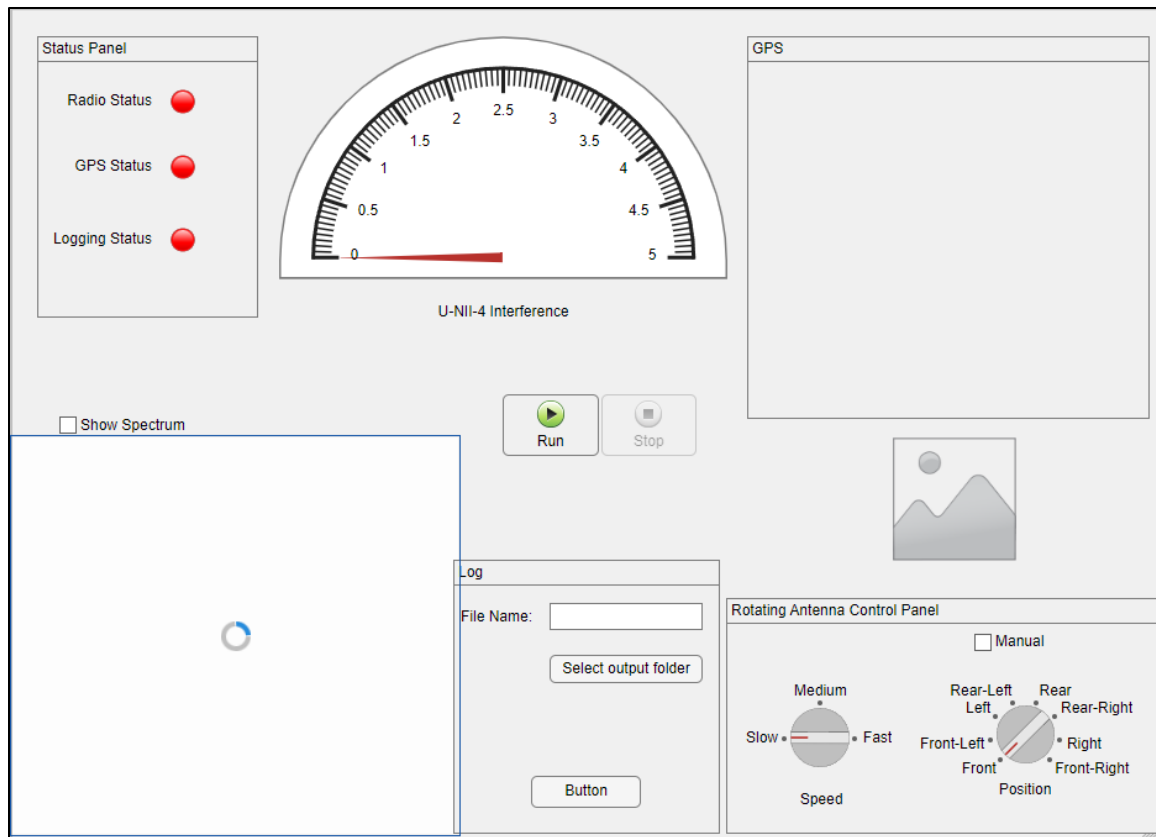


Figure 26. Photo. Version 0.2 of estimator software.

Bigger additions such as a built-in working GPS and a map to indicate where the user was, and a gauge to read the amount of U-NII-4 interference. The GPS uses a GPS receiver to transmit NMEA sentences to the GUI. Thankfully, MATLAB has a built-in function to take the NMEA string and translate it into a longitude and latitude. For the gauge the research team used data from the Simulink module that computes an estimate of interference.

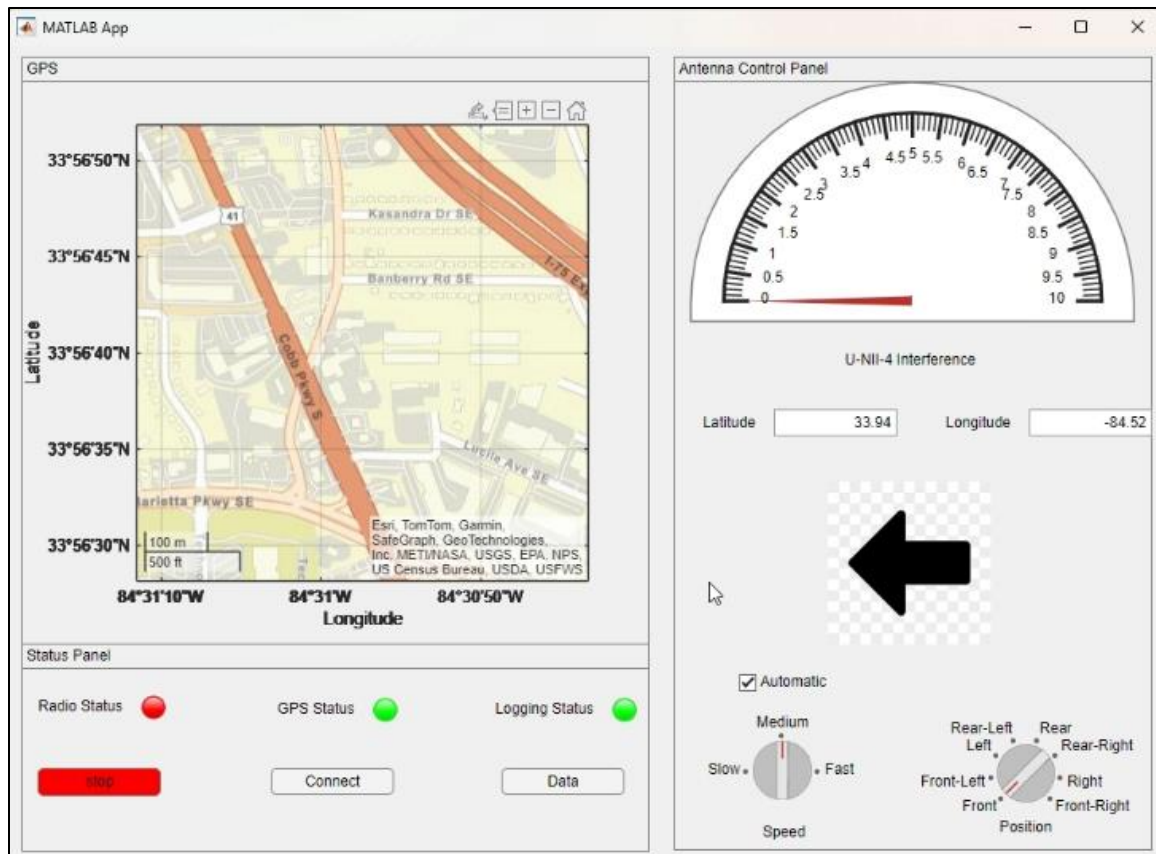


Figure 27. Photo. Version 0.6 with GPS working.

At this point most of the app's functionality was complete. Only a few major features remained to be implemented. First, logging data for the user, data logging and the data options were placed on a separate screen to not overwhelm the user with so many options. On the data screen the user can input a name for a file, the app will create a text file. Users can allow the app to automatically log data or manually log data through a button. When logging data the app will write the current latitude, longitude, gauge reading, radio direction, and a time stamp in a CSV format.

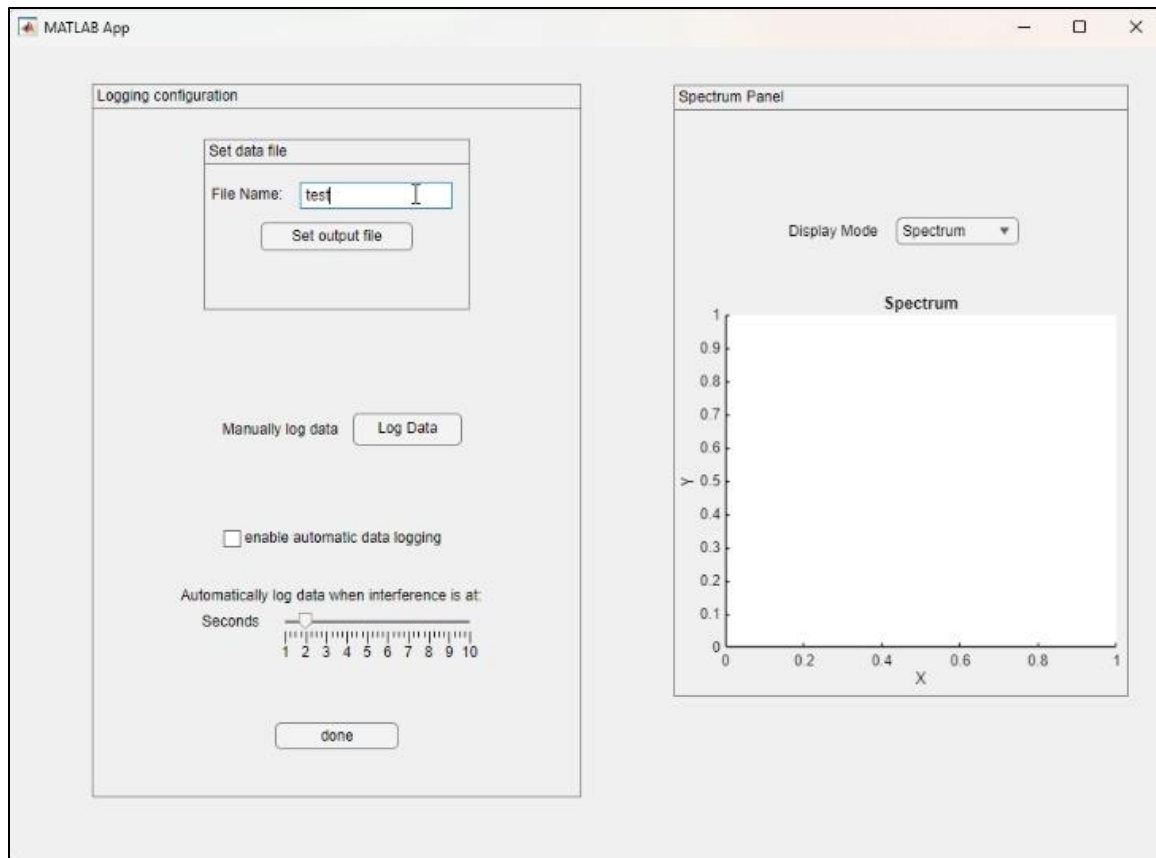


Figure 28. Photo. Version 0.6 showing data screen.

The final implementation was a connection between MATLAB app and the Arduino microcontroller. By using a serial connection, the app can easily connect and send data to control the Arduino code.

ARDUINO CODE

The initial version of the code logic functioned using eight (8) IR sensors. The idea was to enumerate each of these sensors and assign each a direction (Front – 0, Front-Left – 1, Left – 2, Rear-Left – 3, Rear – 4, Rear-Right – 5, Right – 6, and Front-Right – 7). Using several functions in the code, theoretically could start and stop the antenna, increase and decrease the speed of the antenna, passively read signals (continuously), and direct the antenna to

the desired direction using the sensors (manual). While the other functions worked perfectly, there was difficulty in operating manually. The way the manual function was expected to work was that after receiving an input from the user on the MATLAB GUI, it would spin the antenna until it reached the desired location. This desired location would be identified by the code by the antenna spinning until the IR beam of the desired sensor was broken, prompting the rotation to instantaneously stop. Issues were present in three main forms: the logic to operate the manual function was contradictory to the other functions, faulty or damaged IR sensors made it challenging, and even when rotating, the antenna would always take the longest path to find the desired input.

To resolve this, the general logic was remade to use only one IR sensor. This IR sensor now serves as the origin point (Front – 0), and from there only have the following functions:

- ***startPosition***: Rotates the antenna until the origin IR beam is broken and the motor stops. This function is also present in the setup function, meaning that it always happens upon initiation of the program.
- ***serialCommand***: This function operates the receiving the targetValue input that are simply number inputs, (0 – 7) that direct the antenna in the desired direction.
- ***antennaMove***: This function operates the movement of the antenna to desired locations. It takes the target position (targetValue) and the uses the current position (intitalValue) and performs calculations to decide the next move.
 - (*intitalValue* < *targetValue*): the code will subtract intitalValue from targetValue then is multiplies by 50 to give the number of steps needed to move.

- (*intitalValue* < *targetValue*): the code will subtract *targetValue* from *intitalValue* then once that value has been multiplied by 50 it will be subtracted from 400 (total steps for a full rotation) to give the number of steps needed to move.

RESULTS

After four months of slow progress, the app reached a point where the team could confidently call it version 1.0, as it now had the full functionality that was needed. The code has been vastly simplified to allow for easier manipulation by the user. It allows the MATLAB GUI to control speed input and directional output flawlessly. With fewer functions in the Arduino code, potential changes can now be made more easily to suit the user's needs. Additionally, the user interface of the MATLAB GUI offers the user a streamlined experience.

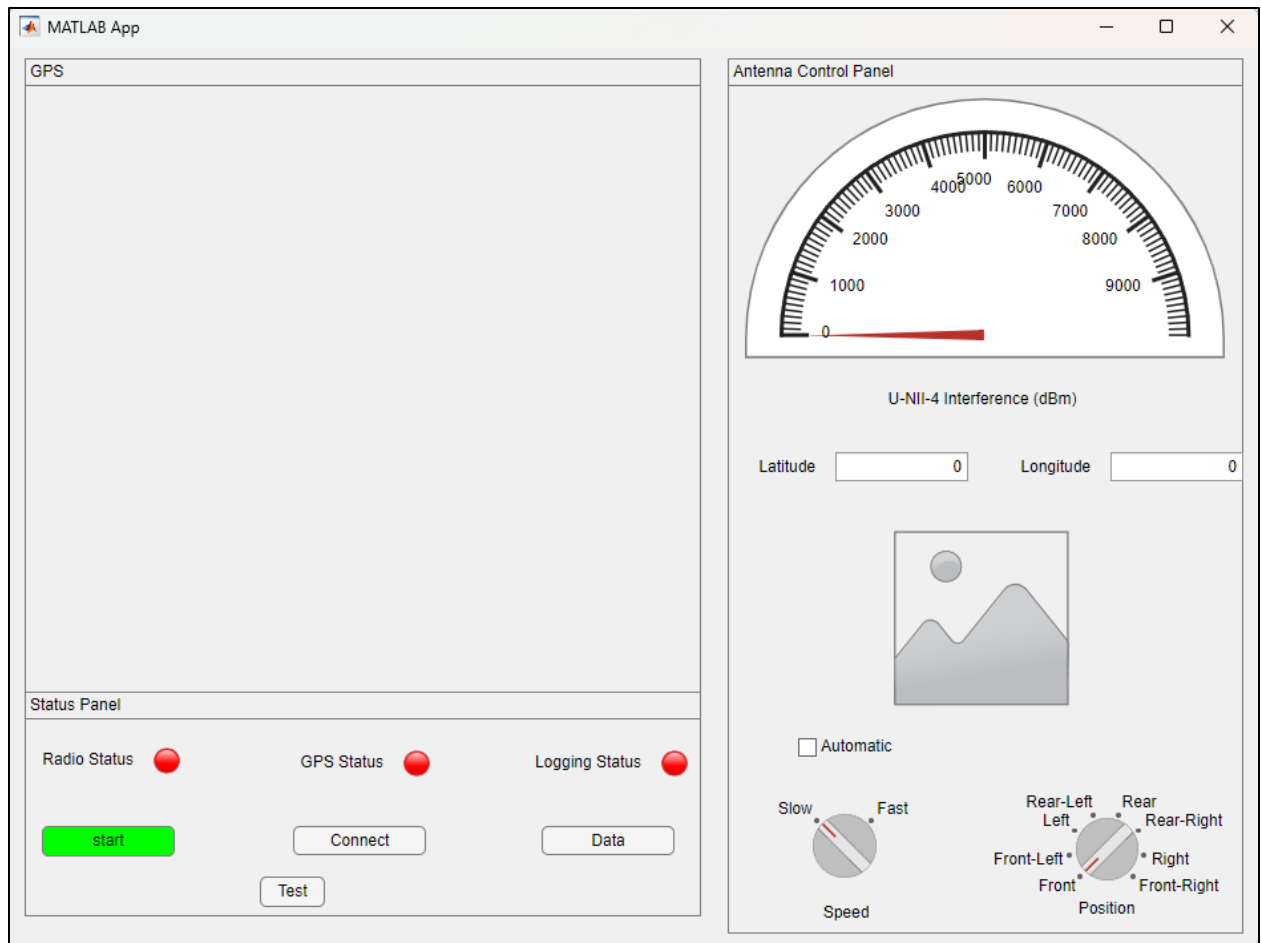


Figure 29. Photo. Version 1.0 main screen

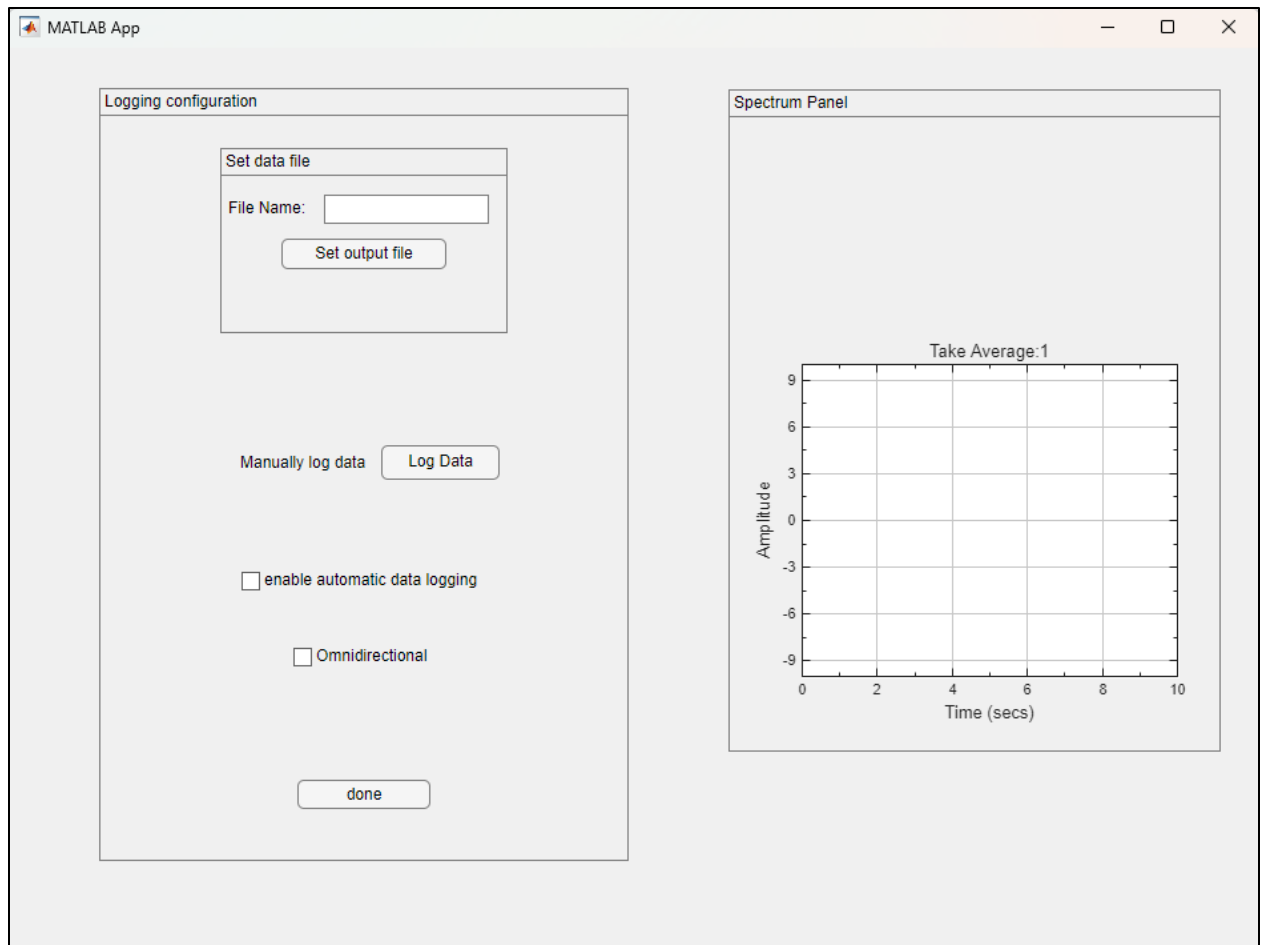


Figure 30. Photo. Version 1.0 data screen.

APPENDIX C. IN-LINE RF HARDWARE BOM

- 2x 20 dB attenuators (with SMA connectors)
- 2x three-port RF circulators for 5.9GHz (with SMA connectors)
- 1x short RF cable SMA
- 1x N-TYPE MALE to SMA adapter
- 1x N-TYPE FEMALE to SMA adapter

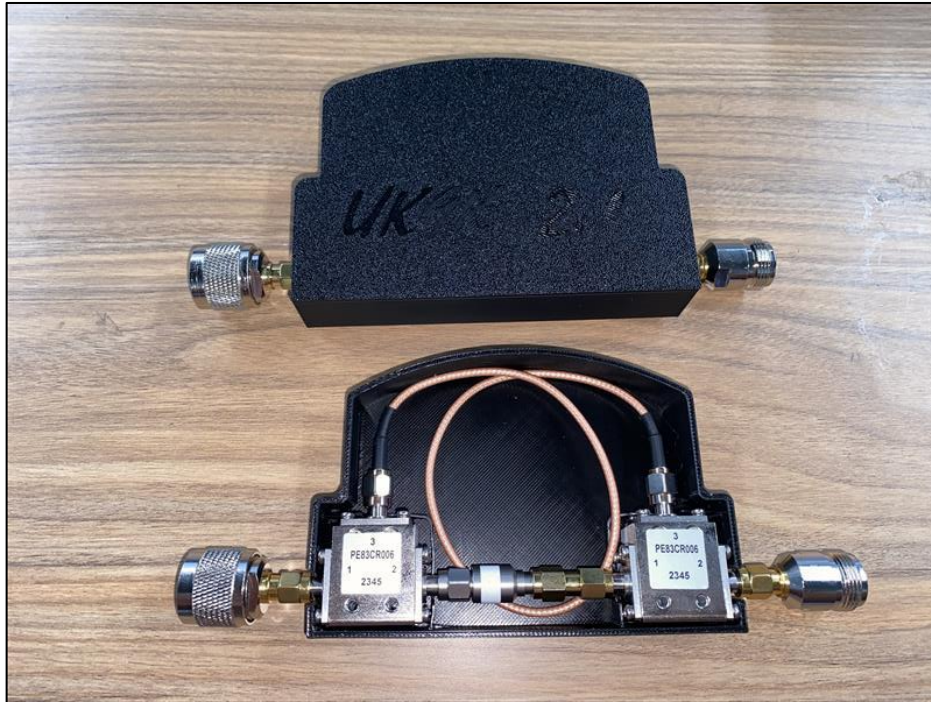


Figure 31. Photo. Assemble according to this configuration in a 3D printed case.

ACKNOWLEDGMENTS

The success of this research would not have been possible without the support of several individuals. The team would like to thank the Georgia Department of Transportation (GDOT) for their financial support and involvement during this research study. Specifically, the research team thanks: Alan Davis, GDOT State Traffic Engineer; Justin Hatch, GDOT Assistant State Traffic Engineer; Victoria Coulter, GDOT State Signal Operations Engineer; Purser Sturgeon II and Colby Inman for access to the roadside unit logs, Erica Depaula for loaning the research team a real-time spectrum analyzer, and the restaurant owners and management for allowing use of their outdoor deck during field experiments. The food was also splendid. Additionally, the researchers wish to thank KSU post-award specialist Ann Graham and GDOT Research Program Manager Brennan A. Roney for ensuring the project accounting stayed accurate and on-track. Lastly, the PI would like to personally thank his Lord and Savior Jesus Christ for helping with the research, the students who participated in the work, and his family and colleagues for their continued support!

REFERENCES

1. B. Kihei, C. Barclay and J. Greaves-Taylor, "5.9GHz Interference Resiliency for Connected Vehicle Equipment," FHWA, Atlanta, GA, 2023.
2. Federal Communications Commission, "Use of the 5.850-5.925 GHz Band," FCC, Washington, D.C., 2024.
3. Federal Communications Commission, "ORDER ON RECONSIDERATION," 2024.
4. Federal Communications Commission, "Use of the 5.850-5.925 GHz Band," 2021.
5. Federal Communications Commission, "47 CFR § 2.106".
6. Federal Communications Commission, "Fcc table of frequency allocations," 2024.
7. K. Sheriff, H. Moelterm, J. Jandura and E. Kuka, "FCC Approves C-V2X Technology for Connected Vehicles Ahead of Final ITS Rules," 2023.
8. US Department of Transportation, "Recent FCC Public Notices on the 5.9 GHz Safety Band," 2022.
9. U.S. DEPARTMENT OF COMMERCE, "United States Frequency Allocations The Radio Spectrum," 2016.
10. J. Peha, "Spectrum for Connected Vehicles," 2020 Mobility21 UTC, 2020.
11. J. Peha, "Rethinking Connected Vehicles for Spectrum Scarcity," 2020 Mobility21 UTC, FAST Act – Mobility National, 2020.
12. S. Kuciemba, "Evaluation and Synthesis of Connected Vehicle Communication Technologies," AASHTO, WSP USA, 2020.
13. S. Kuciemba, T. Timcho, M. McLaughlin and F. Perry, "V2X COMMUNICATIONS IN THE 5.9 GHZ SPECTRUM: NEW DIRECTIONS, OPPORTUNITIES, AND CHALLENGES," WSP USA, 2021.
14. T. Stone, "EXCLUSIVE: THEA testing for V2X interference in 5.9GHz band," trafficechnologytoday.com, 2021.

15. S. VanSickle, F. Ahmed-Zaid, H. Krishnan, T. Khatchatrian, S. Mahmud, E. Moradi-Pari, N. Probert, S. Ahmad, S. Kamthan, B. Gallagher and J. McNew, "Vehicle-to-Vehicle Communications Research Project (V2V-CR) DSRC and Wi-Fi Baseline Cross-channel Interference Test and Measurement Report," NHTSA, NHTSA, 2019.
16. US DOT, "Preliminary Testing: Out-of-Channel Interference (Out-of-Band Emissions)," US DOT, 2019.
17. CAMP LLC, "Task 8: Assessment of WiFi Interference to C-V2X Communication Based on Proposed FCC 5.9 GHz NPRM," 2020.
18. G. Naik and J. Park, "Impact of Wi-Fi Transmissions on C-V2X Performance," IEEE, 2019.
19. P. Kurumpanai and B. Kihei, "OwlBox: A Comparison of Processor Architecture and Software Runtime on Vehicle-to-Everything Communication for Intelligent Transportation Systems," IEEE, Atlanta, 2022.